Supplementary Information

Observation of Binding and Rotation of Methane and Hydrogen within a Functional Metal-Organic Framework

Mathew Savage,[1] Ivan da Silva,[2] Mark Johnson,[3] Joseph H. Carter,[4] Ruth Newby,[4] Mikhail Suyetin,[4] Elena Besley,[4] Pascal Manuel,[2] Svemir Rudić,[2] Andrew N. Fitch,[5] Claire Murray,[6] William I.F. David,[2] Sihai Yang[1]* and Martin Schröder[1]*

[1] School of Chemistry, University of Manchester, Chemistry Building, Manchester, M13 9PL (UK)

Tel: +44 (0)161 306 9119; Sihai.Yang@manchester.ac.uk; m.schroder@manchester.ac.uk

[2] ISIS Facility, STFC Rutherford Appleton Laboratory, Chilton, Oxfordshire, OX11 0QX (UK)

[3] ILL Neutron Facility, Grenoble, 38043 (France)

[4] School of Chemistry, University of Nottingham, University Park, Nottingham, NG7 2RD (UK)

[5] European Synchrotron Radiation Facility, Grenoble, 38043 (France)

[6] Diamond Light Source, Harwell Science Campus, Oxfordshire, OX11 0DE (UK)

Contents

Materials and measurements

All reagents and solvents were purchased from commercial suppliers and used without further purification. Elemental analyses (C, H and N) were carried out on a CE-440 elemental analyser. Thermal Gravimetric Analysis (TGA) was performed under nitrogen or synthetic air flow (100 ml/min) with a heating rate of 5°C/min using a Perkin-Elmer Pyris 1 Thermogravimetric Analyser. Fourier Transform (FTIR) spectra were recorded using a Nicolet Avatar 360 FT-IR spectrometer in the 4000~400 cm^{-1} range with an iD5 ATR accessory. Powder X-Ray Diffraction (PXRD) data were collected in flat plate mode over the 2θ range 5-50° on a PANalytical X'pert MultiPurpose Diffractometer using Cu-K_α radiation (λ = 1.54056 Å) at 40 kV and 40 mA.

Synthesis of MFM-300(In)

H_4L (330 mg, 1.00 mmol), $In(NO_3)_3 \cdot 5H_2O$ (585 mg, 1.50 mmol) were mixed and dispersed in a DMF/MeCN mixture (30 ml, 2:1 v/v) in a 250 mL glass pressure reactor. The white slurry was acidified with conc. nitric acid (65% 1.0 mL), the vessel sealed and heated at 80 °C for 48 h. The resultant flaky white precipitate was then washed with DMF and dried briefly in air. Yield 347 mg (42 % yield based upon solvent content from microanalysis). Elemental analysis $[In_2(OH)_2(C_{16}H_6O_8)] \cdot 1.28H_2O \cdot 2.87(C_3H_7NO)$ (% calc/found) C 35.92/35.92, H 3.75/3.53, N 4.88/4.88.

The acetone-exchanged material was prepared by suspending the as-synthesised sample in an excess of acetone for 5 days with frequent exchange of solvent. Elemental analysis $[In_2(OH)_2(C_{16}H_6O_8)] \cdot 1.10H_2O \cdot 1.76(C_3H_6O)$ (% calc/found) C 35.91/35.91, H 2.94/2.94, N 0.00/0.00. Selected IR(ATR): ν/cm^{-1} = 3501 (br), 1705 (s), 1610 (s), 1550 (br), 1418 (br), 1359 (s), 1220 (s), 1089 (w), 782 (s), 748 (s).

Powder X-Ray Diffraction (PXRD) measurements

Powder X-Ray Diffraction patterns were collected for both the as synthesised and acetone exchanged material and show a flat background, with a low amorphous content and sharp peaks. Pawley fits of the diffraction patterns were calculated with the Bruker TOPAS software suite and are shown to be a good match with the experimental measurement with low residuals and no un-indexed peaks. The calculated unit cell parameters are consistent with those derived from the single crystal experiment.

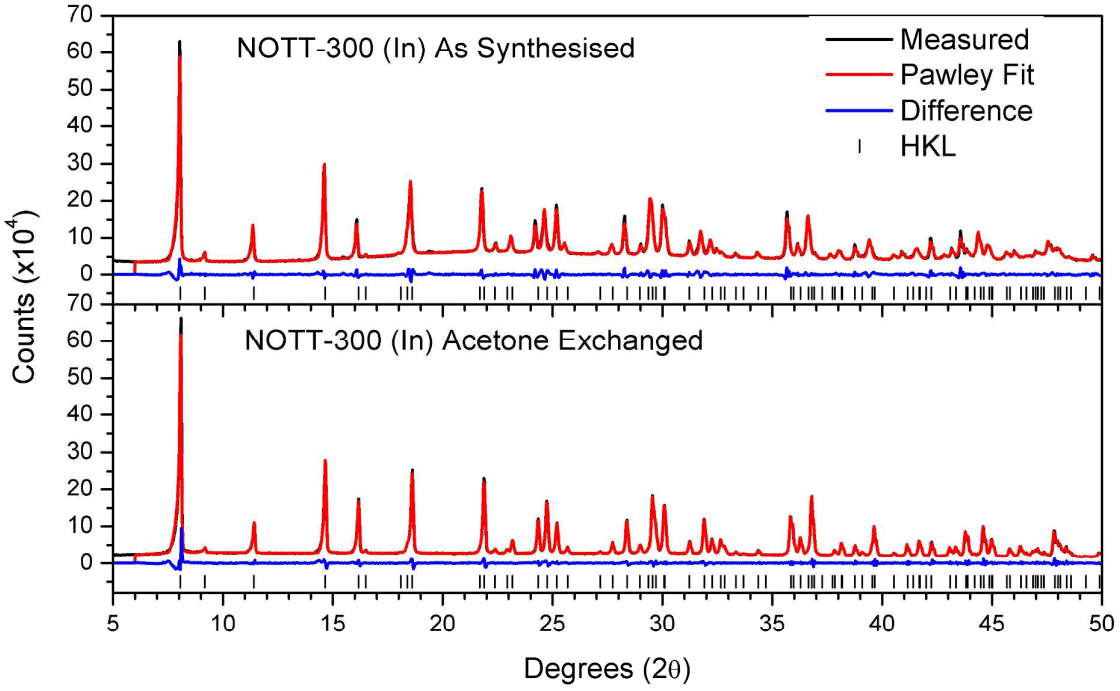

Figure S1 PXRD patterns of as-synthesised and acetone-exchanged MFM-300(In)

High Resolution Synchrotron X-Ray Powder Diffraction

High resolution synchrotron X-ray powder diffraction (PXRD) data were collected at Beamline ID31 of the ESRF [λ = 0.49589(2) Å] and I11 of Diamond Light Source using multi-analysing crystal-detectors (MACs)[1] and monochromated radiation [λ = 0.827136(2) Å]. The powder sample of MFM-300(In) was dried in air and ground for 10 min before loading into a capillary tube (0.7 mm diameter). The powder pattern was first indexed on a body-centred tetragonal lattice and the independent unit cell parameters were refined using TOPAS. The structure solutions were initially established by considering the structure of the MFM-300(Al) framework with an expansion of unit cell volume of ~15% ongoing from Al to In, and the residual electron density maps were further developed from subsequent difference Fourier analysis using TOPAS. The final structure refinement of MFM-300(In) was carried out using the Rietveld method[2] with isotropic displacement parameters for all atoms. The highly disordered solvent molecules (DMF, CH_3CN and water) in the pores could not be located and modelled, and therefore were treated as discrete water molecules in the refinement. A total of 40 disordered water molecules per unit cell were found within the channels and included in the final structure refinement for MFM-300(In)-solv. The final stage of the Rietveld refinement involved soft restraints to the C-C bond lengths within the benzene rings and carboxylate groups.

Crystal data for MFM-300(In)-solv: $[In_2(OH)_2(C_{16}H_6O_8)](H_2O)_5$. White powder. Tetragonal, space group $I4_122$, $a = b = 15.55796(3)$, $c = 12.31160(2)$ Å, $V = 2980.02(1)$ Å^3, $M = 679.9$, $T = 273(2)$ K, Z = 4. The final Rietveld plot corresponds to satisfactory crystal structure model ($R_{Bragg} = 0.036$) and profile ($R_p = 0.054$ and $R_{wp} = 0.072$) indicators with a goodness-of-fit parameter of 2.41.

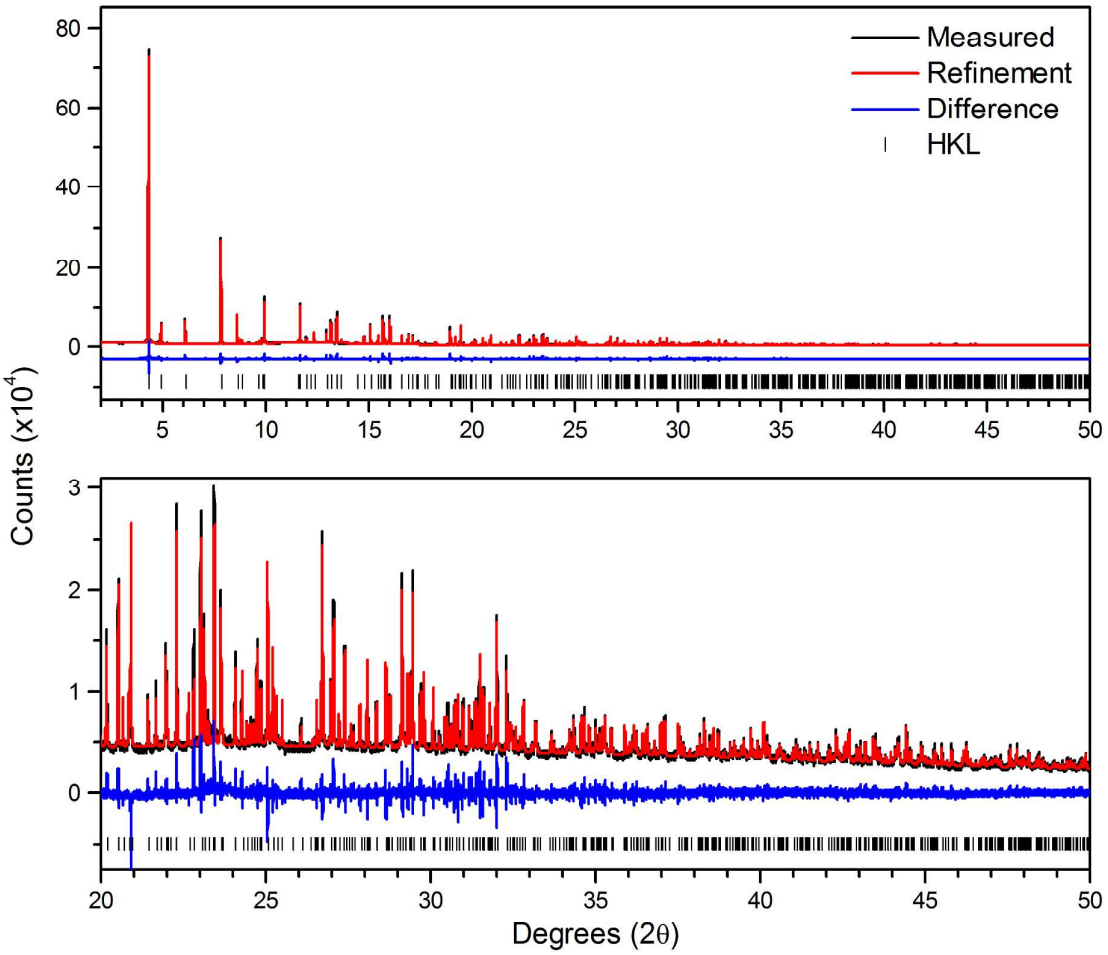

Figure S2 PXRD patterns [observed (black), calculated (red) and difference (blue)] for the Rietveld refinement of the as-synthesised MFM-300(In) [λ = 0.827136(2) Å]; Top full data range, Bottom, high angle data (2θ = 20-50^{o}) scaled up to show the quality of fit between the observed and the calculated patterns.

Additional Crystal Structure Views

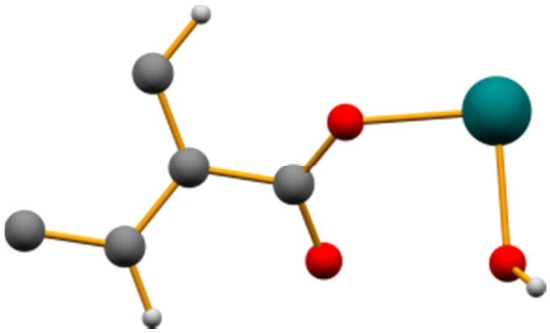

Figure S3 View of the asymmetric unit of MFM-300(In)

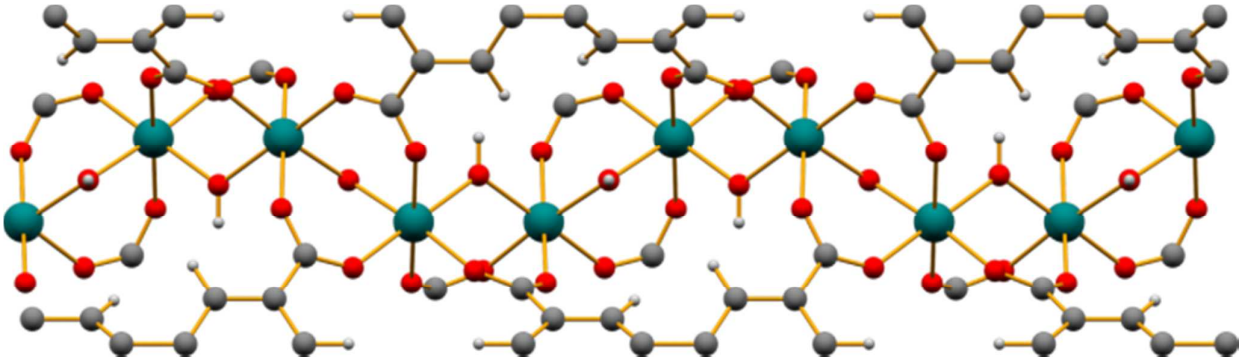

Figure S4 View of the indium oxide chain of MFM-300(In)

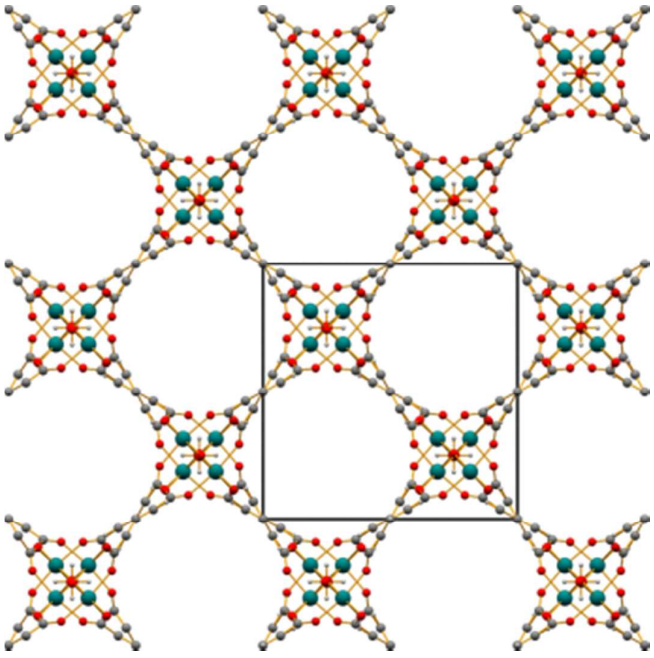

Figure S5View of extended framework of MFM-300(In) down the c axis showing the unit cell.

Thermal Gravimetric Analysis (TGA) Measurements

The uncoordinated solvent molecules in MFM-300(In) can be readily exchanged for acetone and removed by heating at 120 °C either under a flow of N_2 gas or *in vacuo*. TGA measurements show that the as synthesised sample loses solvent slowly between 35 and 300 °C, while the acetone-exchanged sample loses solvent rapidly between 35 and 200 °C, giving the fully desolvated material MFM-300(In). This is followed by a significant loss at *ca*. 400 °C, corresponding to the decomposition of the framework.

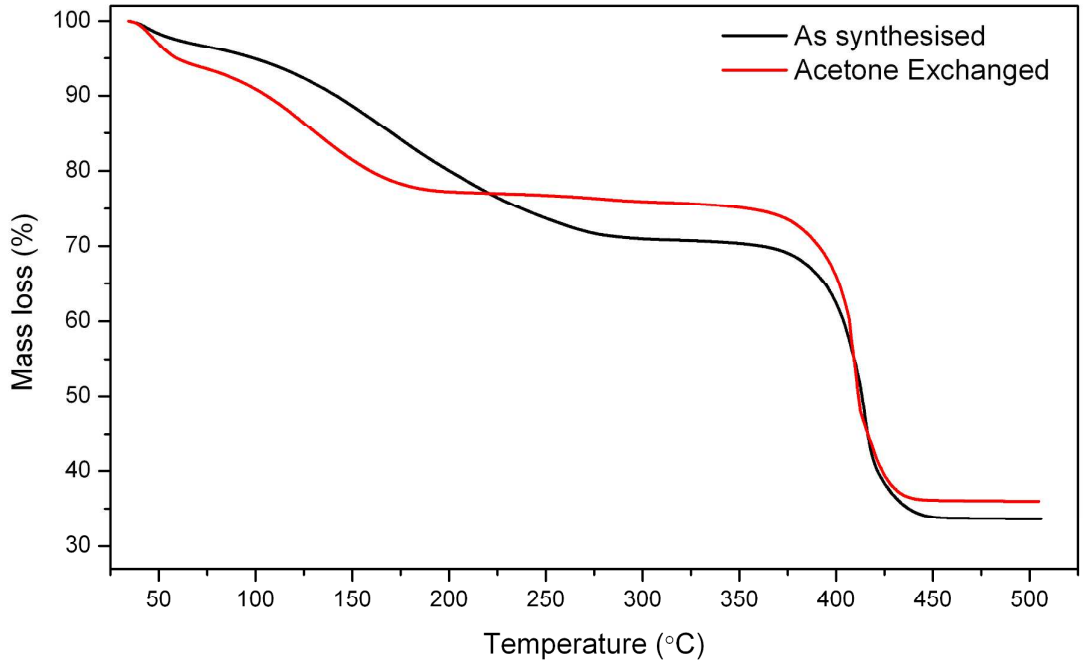

Figure S6 Comparison of TGA plots for as synthesised MFM-300(In) and acetone-exchanged MFM-300(In) under air flows.

Elemental Microanalysis

Calculated solvent content from elemental analysis correlates with TGA mass losses; As synthesised material; $[In_2(OH)_2(C_{16}H_6O_8)]\cdot 1.28H_2O\cdot 2.87(C_3H_7NO)$ (% calc/found) C 35.92/35.92, H 3.75/3.53, N 4.88/4.88. The mass loss of 1.9 wt% between 35 and 100 °C correlates to 1.27 H_2O molecules while the mass loss of 26.5 wt% between 100 and 300 °C correlates with the loss of 2.9 DMF molecules.

Acetone exchanged material; $[In_2(OH)_2(C_{16}H_6O_8)]\cdot 1.10H_2O\cdot 1.76(C_3H_6O)$ (% calc/found) C 35.91/35.91, H 2.94/2.94, N 0.00/0. The mass loss of 5.4 wt% between 35 and 100 °C corresponds to the loss of 0.92 acetone molecules, while the mass loss of 18.8 wt% between 100 and 200 °C corresponds to 1.73 acetone and 1.12 H_2O molecules.

A sample of the acetone exchanged material was degassed at 120 °C and 1 x 10^{-6} mBar for 20 hours to give a dry, desolvated material. This was then exposed to the atmosphere before loading into the elemental analyser; $[In_2(OH)_2(C_{16}H_6O_8)]\cdot 0.73H_2O$ (% calc/found) C 31.87/31.87, H 1.58/1.32, N 0/0. The presence of atmospheric H_2O indicates that the acetone solvent can be removed under these conditions.

Material	Calculated			Experimental		
	C	H	N	C	H	N
$[In_2(OH)_2(C_{16}H_6O_8)]\cdot 1.28H_2O\cdot 2.87(C_3H_7NO)$	35.92	3.75	4.88	35.91	3.53	4.88
$[In_2(OH)_2(C_{16}H_6O_8)]\cdot 1.10H_2O\cdot 1.76(C_3H_6O)$	35.91	2.94	0	35.91	2.94	0
$[In_2(OH)_2(C_{16}H_6O_8)]\cdot 0.73H_2O$	31.87	1.58	0	31.87	1.32	0

Table S1 Calculated and experimental elemental analytical data for as-synthesised, acetone exchanged and desolvated MFM-300(In).

Gas Adsorption Measurements

Medium pressure (0 – 20 bar) gravimetric gas adsorption and desorption data were collected using an IGA-003 system (Hiden Isochema, Warrington, UK) equipped with a turbomolecular pumping system backed by a diaphragm pump. H_2 isotherms (0-20 bar) were recorded at 77 and 87 K using liquid nitrogen and argon respectively. CH_4 isotherms (0-20 bar) were recorded at 110, 215 and 245 K by a liquid nitrogen cryo-furnace, 195 K by dry ice/acetone, 273, 283, 293, 303, and 308 K by a temperature controlled water-bath. High pressure (0 – 50 bar) gravimetric gas adsorption and desorption data were collected using a Xemis system (Hiden Isochema, Warrington, UK) equipped with a turbomolecular pumping system backed by a diaphragm pump. CH_4 isotherms (0 – 50 bar) were recorded at 273, 283, 293, 298 and 303 K using a temperature controlled water-bath.

The kinetic profile of each adsorption or desorption step was monitored by the system software from 2 minutes after each pressure has been achieved, and data collected until an exponential model indicated that 99% of the expected equilibrium has been achieved. Typically all adsorption steps reached the 99% adsorption criterion within 5 minutes of the pressure being achieved. The experimentally measured excess adsorption values were converted into the total adsorption values by applying a correction for the buoyancy of the adsorbent, sample cell and adsorbed gas. The buoyancy correction was applied using system software included with the gas adsorption apparatus, taking into account the density and mass of all components of the balance including hang-downs, sample holder, sample and counterweight and correcting for the density of the adsorbate gas using values from the NIST REFPOP database.

Acetone exchanged samples were loaded into the system and degassed at 120 °C and 1 x 10^{-6} mbar for 20 hours to give a dry, desolvated material of typical mass *ca.* 80 mg. Research grade N_2 was purchased from BOC and used as received. 99.995+ % grade H_2 and CH_4 was purchased from Air Liquide and used as received.

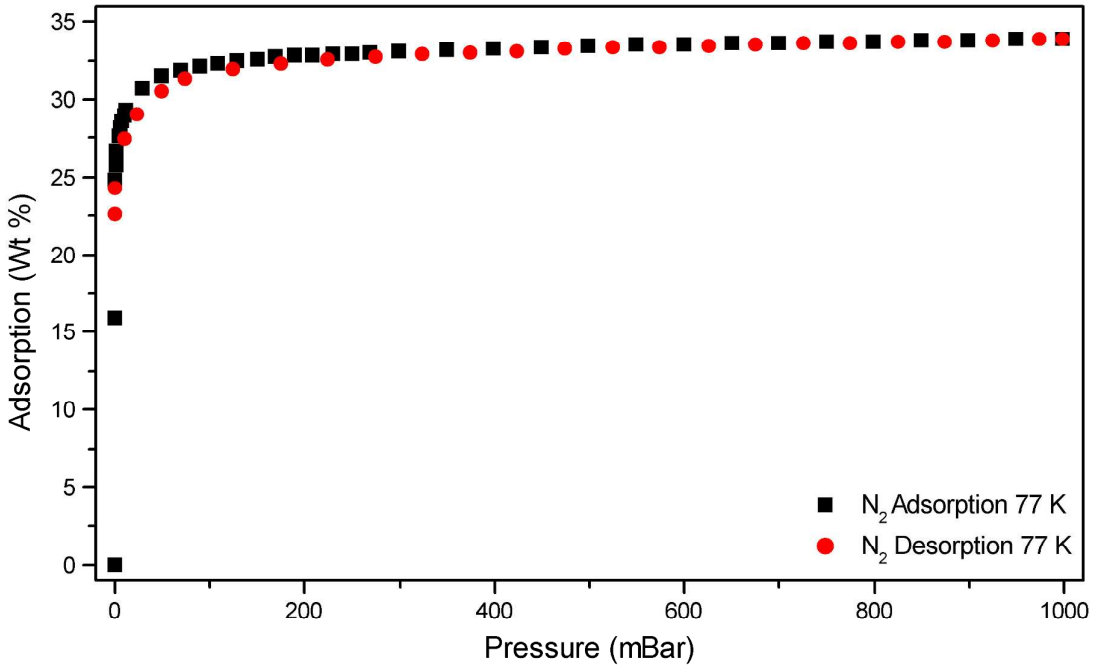

Figure S7 Nitrogen adsorption of MFM-300(In) at 77 K.

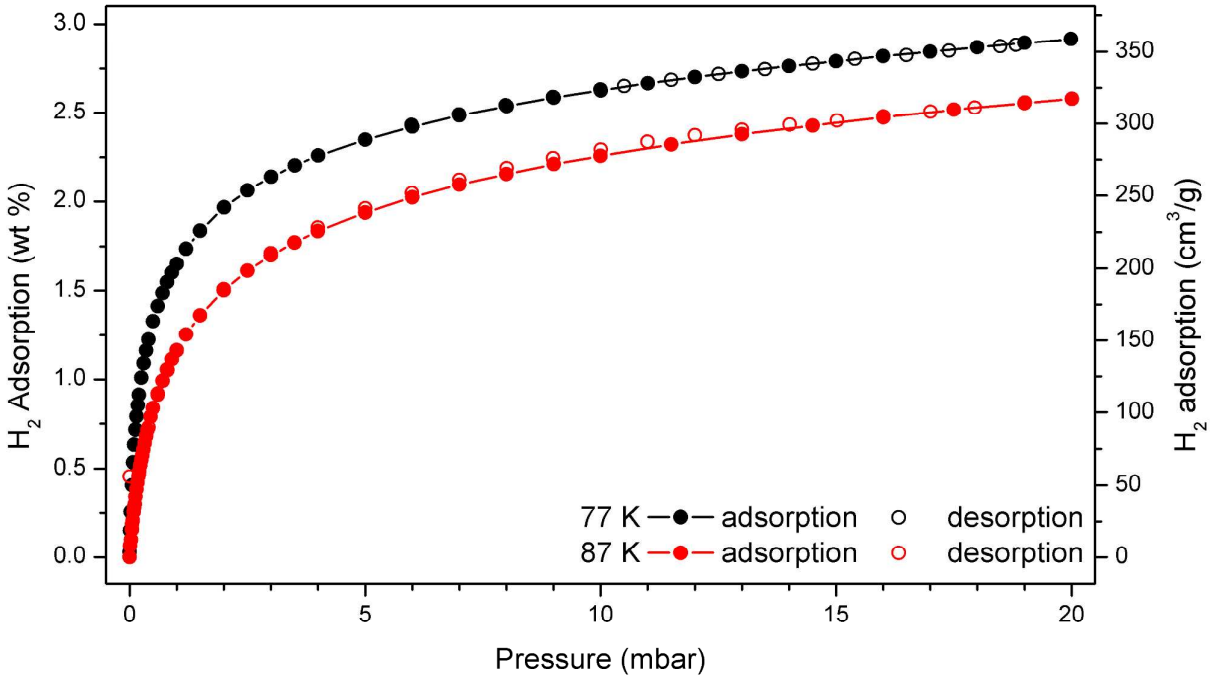

Figure S 8 H_2 adsorption and desorption in MFM-300(In) in terms of wt% and cm^3/g.

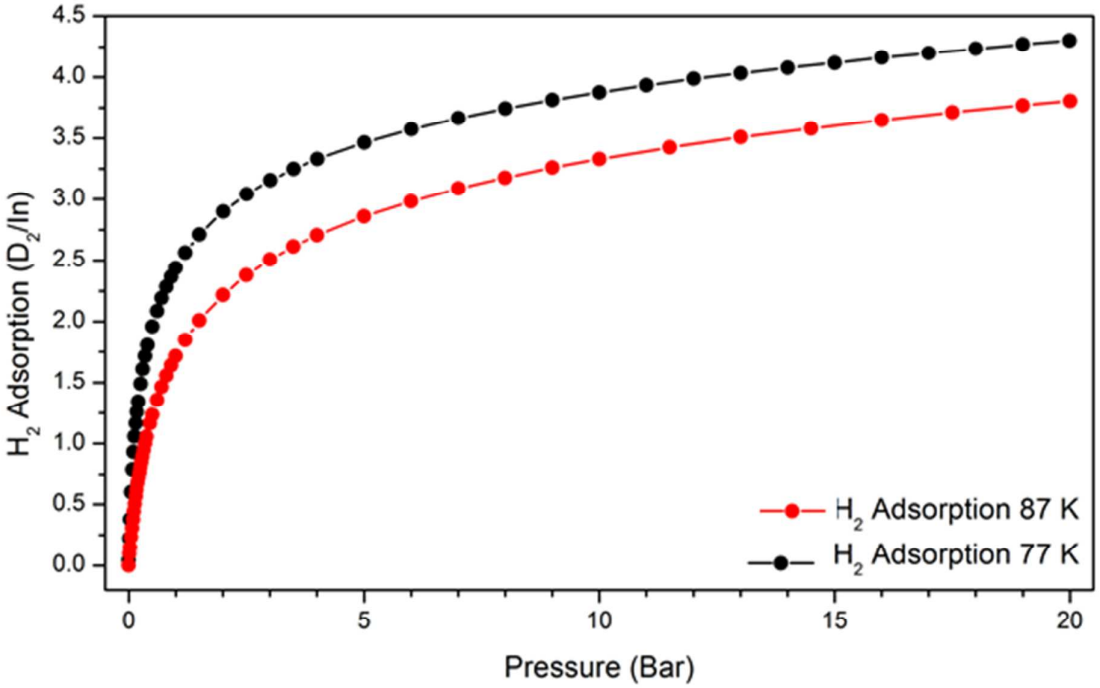

Figure S9 Adsorption of H_2 in MFM-300(In) in terms of H_2 per indium atom.

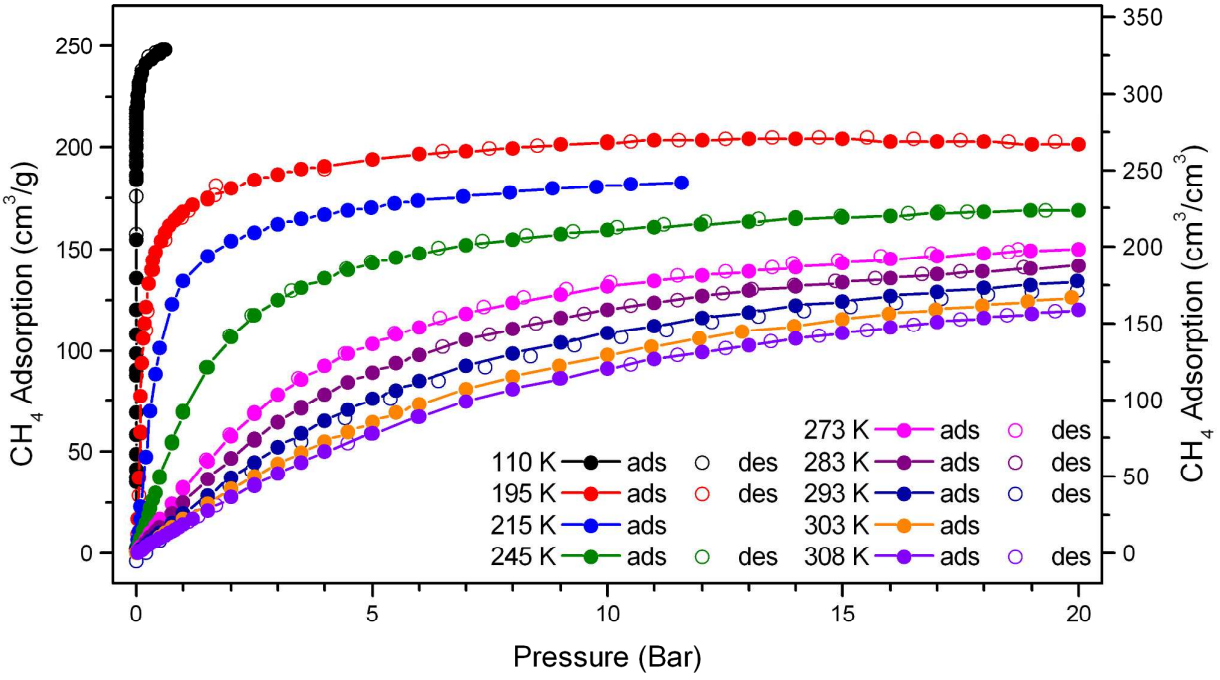

Figure S10 CH_4 adsorption and desorption isotherms in MFM-300(In) in terms of cm^3/g and cm^3/cm^3.

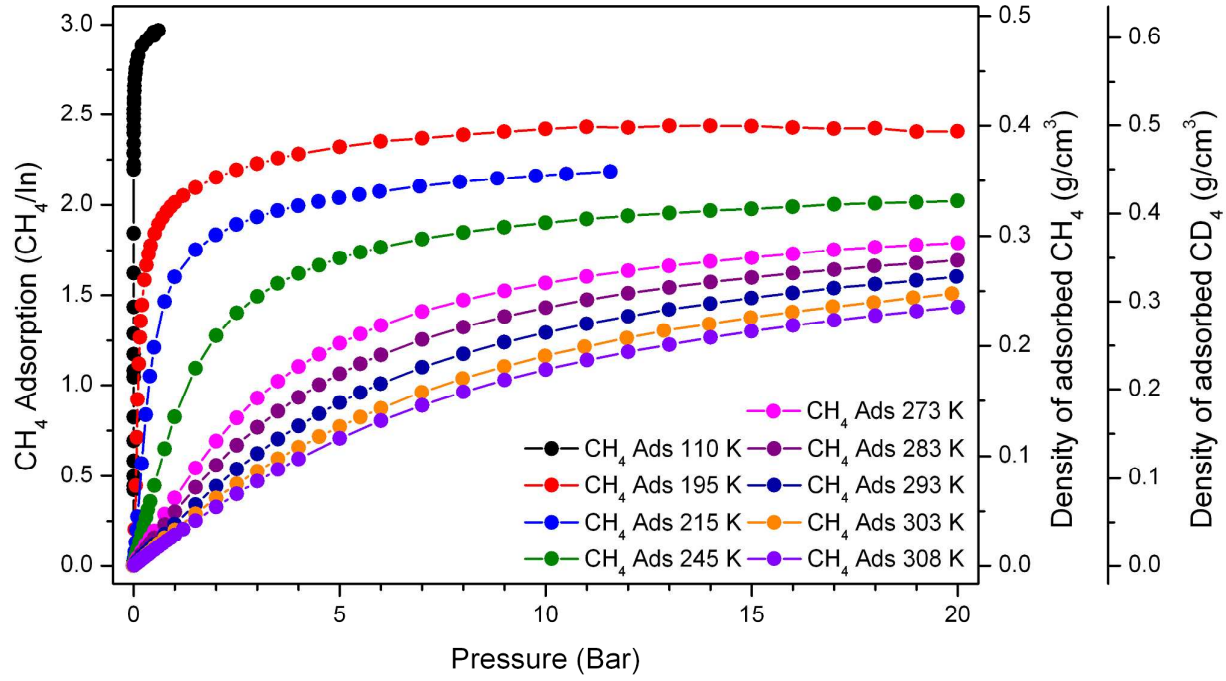

Figure S11 Adsorption of CH_4 in MFM-300(In) in terms of CH_4 per indium atom and the corresponding density of adsorbed CH_4 and CD_4 within the pores of the material.

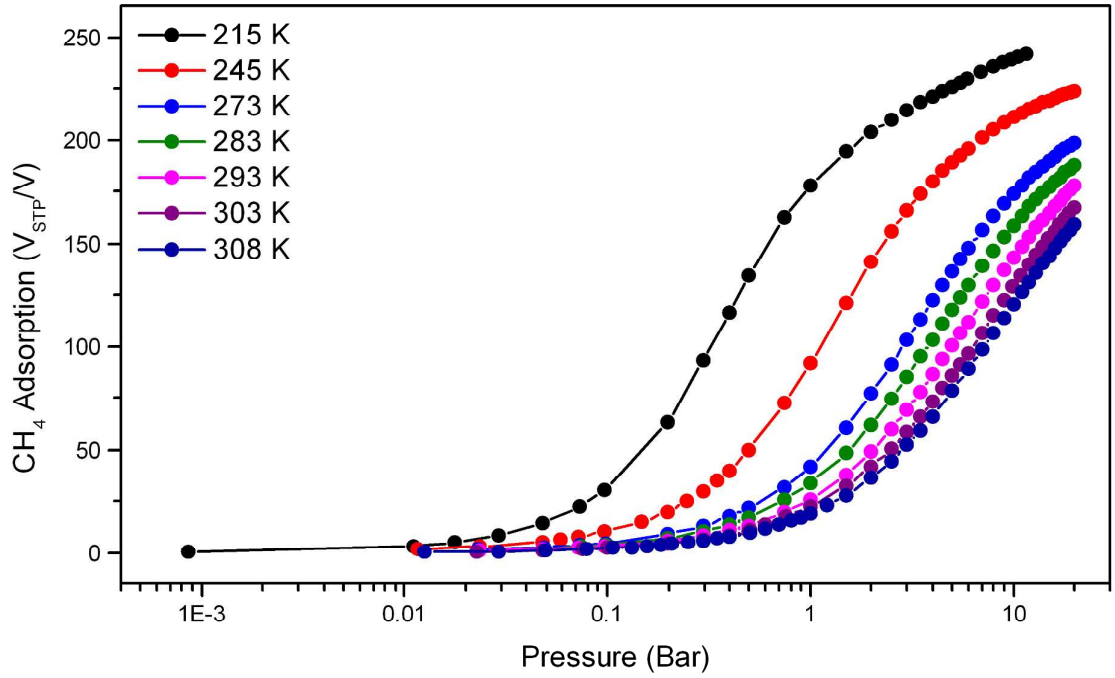

Figure S12 Comparison of the CH_4 adsorption isotherms at 195-308 K of MFM-300(In) in logarithmic view, confirming the absence of distinct adsorption steps

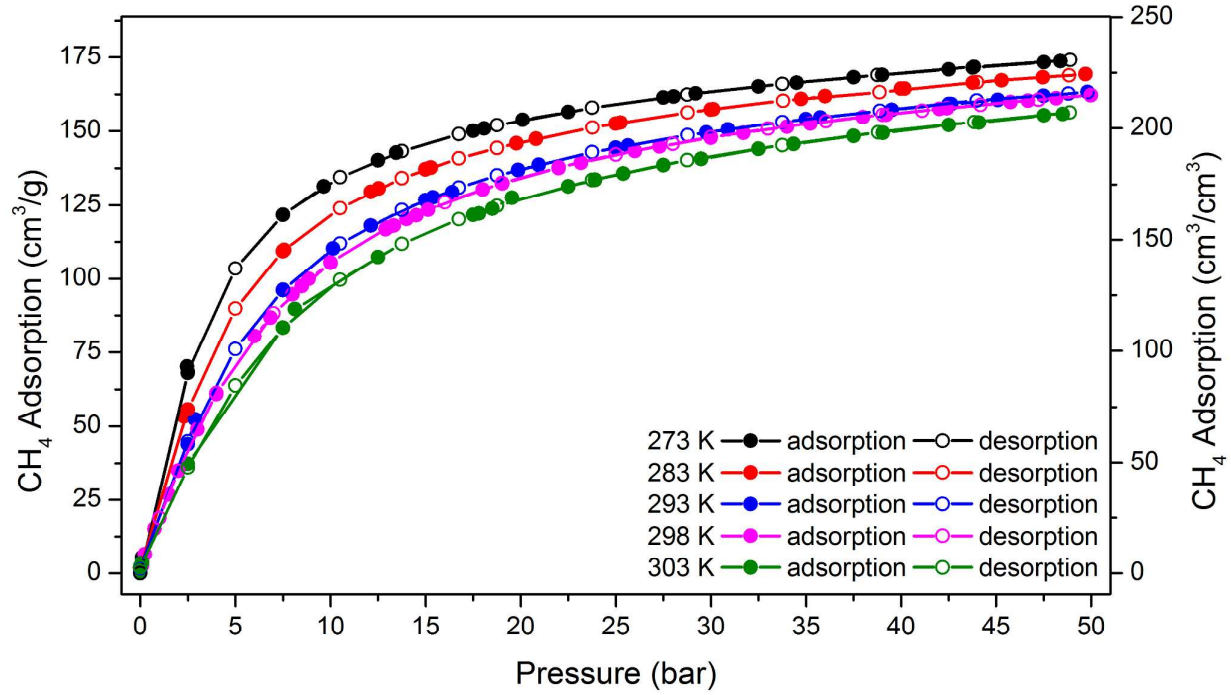

Figure S13 Experimental high pressure (0 – 50 bar) CH_4 adsorption and desorption isotherms in MFM-300(In) in terms of $cm^3\ g^{-1}$ and $cm^3\ cm^{-3}$.

Analysis and Derivation of the Isosteric Heat of Adsorption for H_2

The isosteric enthalpy of adsorption, Q_{st} for hydrogen was determined by fitting the adsorption isotherms at 77 and 87 K to the Virial equation (1);

$$\ln P = \ln n + \frac{1}{T}\sum_{i=0}^{m} a_i n^i + \sum_{j=0}^{n} b_j n^j \qquad (1)$$

Where P is the pressure in millibar, n is the amount of gas adsorbed in mmol/g, T is the temperature in K, a_i and b_j are Virial coefficients and m and n represent the number of coefficients. The global Virial fitting has an R^2 greater than 0.99, indicating the consistency of the isotherm data and the quality of the fit.

The values of the Virial coefficients a_0 through a_m were then used to calculate the isosteric heat of adsorption using equation (2);

$$Q_{st} = -R\sum_{i=0}^{m} a_i n^i \qquad (2)$$

Where Q_{st} is the coverage-dependant isosteric heat of adsorption in KJ mol^{-1} and R is the ideal gas constant.

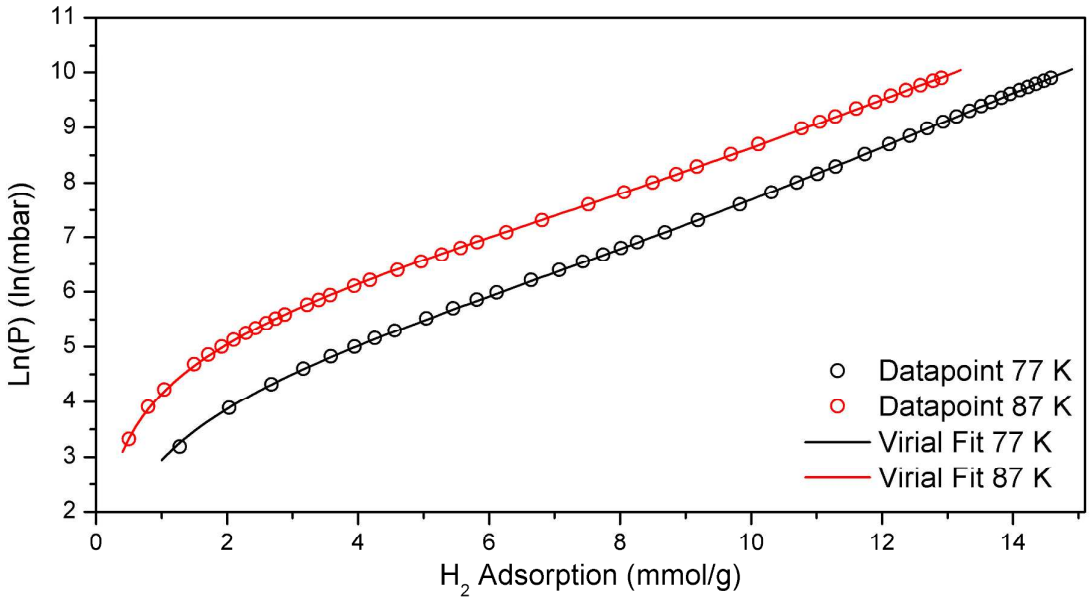

Figure S14 Virial fitting (1) of H_2 adsorption in MFM-300 (In) at 77 and 87 K.

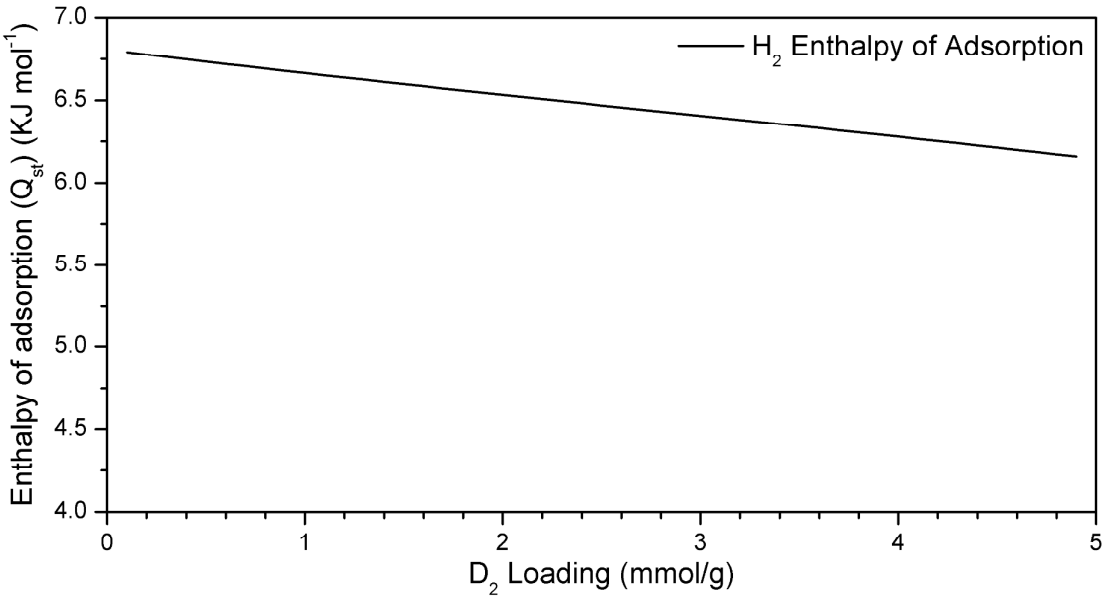

Figure S15 Variation of isosteric enthalpy (Q_{st}) as a function of H_2 loading.

Analysis and Derivation of the Isosteric Head of Adsorption for CH_4

The isosteric enthalpy (ΔH) and entropy (ΔS) for methane was determined by fitting ambient temperature adsorption isotherms to the Van t' Hoff equation **(**3**)** at a number of gas loadings;

$$\ln P = \frac{-\Delta H}{RT} + \frac{\Delta S}{R} \qquad (3)$$

Where *P* is pressure in Pa, T is the temperature, and R is the ideal gas constant. All linear fittings show R^2 above 0.99 indicating the consistency of the isotherm data quality of the fit.

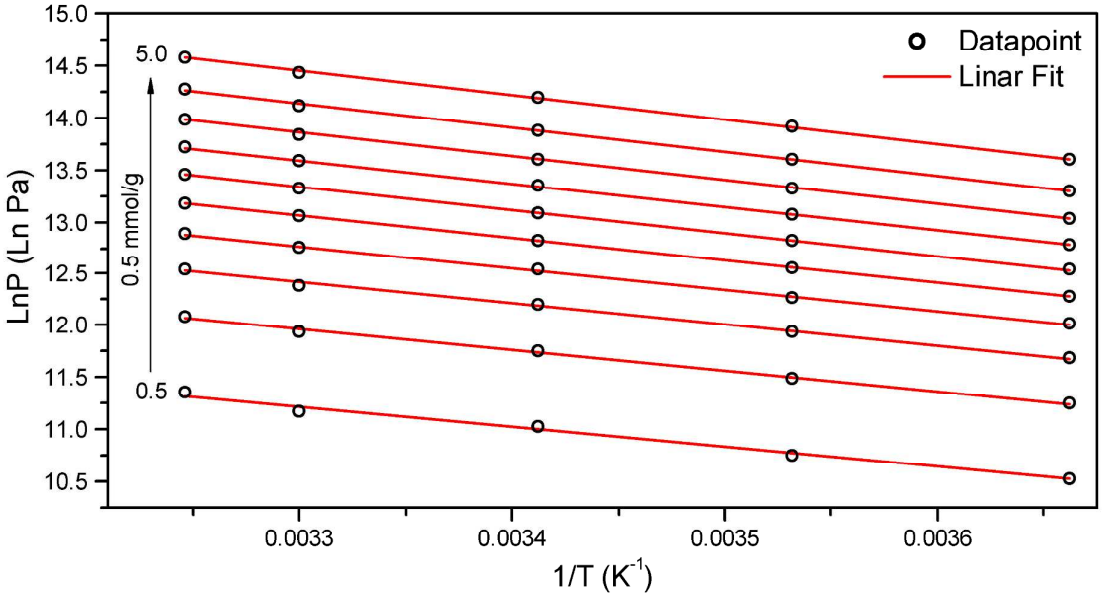

Figure S16 Linear fitting of 1/T vs lnP to determine the isosteric heat of adsorption by the van t' Hoff method.

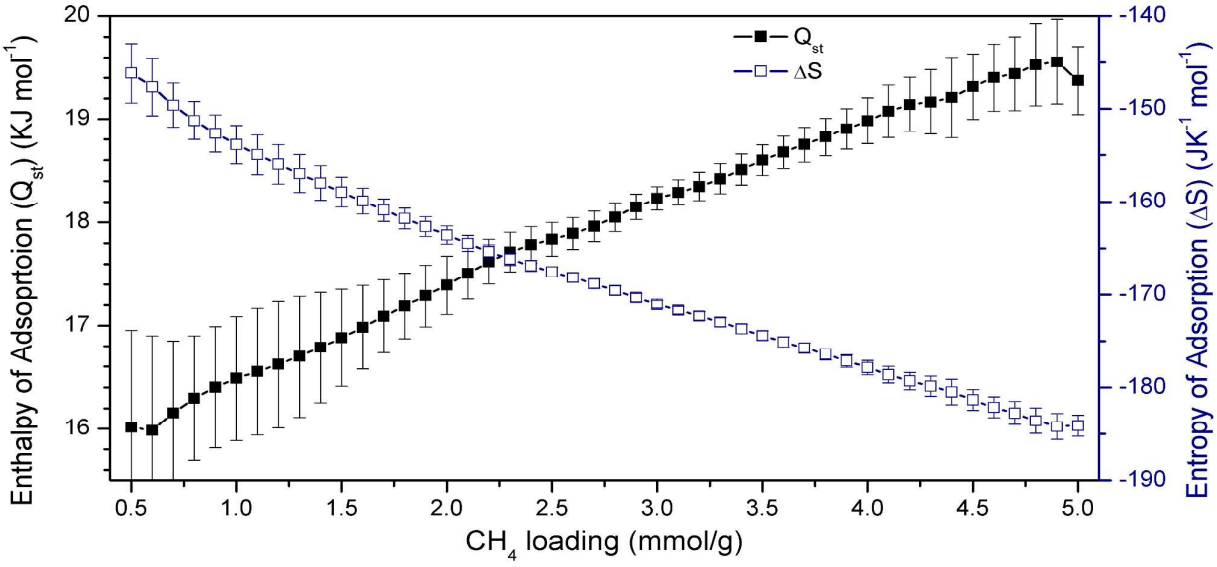

Figure S17 Variation of isosteric enthalpy (Q_{st}) and entropy (ΔS) as a functon of CH_4 loading.

Grand Canonical Monte Carlo (GCMC) Simulations

Grand Canonical Monte Carlo (GCMC) simulations were performed using the MUSIC simulation suite[3] to calculate the adsorption of CH_4 molecules in MFM-300(In). The GCMC simulations involved $3 \cdot 10^6$ steps of equilibration, followed by $3 \cdot 10^6$ steps of the production run. The CH_4 molecule was described by TraPPE force field[4] using a set of united-atom Lennard-Jones interaction parameters σ_O=3.73 Å, ε_O/k_B = 148.0 K. All atoms in the MOF structure were described by the universal force field (UFF)[5] with scaling techniques applied, developed by Perez-Pellitero et al:[6] parameters of MOF atoms for GCMC simulations were scaled: sigma_new = sigma·0.95 and eps_new = eps·0.69. The simulation cell contained 12 (2x2x3) unit cells with periodic boundary conditions. The fugacity has been calculated from the Peng-Robertson equation of state[7] and the MOF and guest molecules were considered to be rigid. A Lennard-Jones potential has been used to describe the van der Waals interactions with a cut-off distance of 12.8 Å.

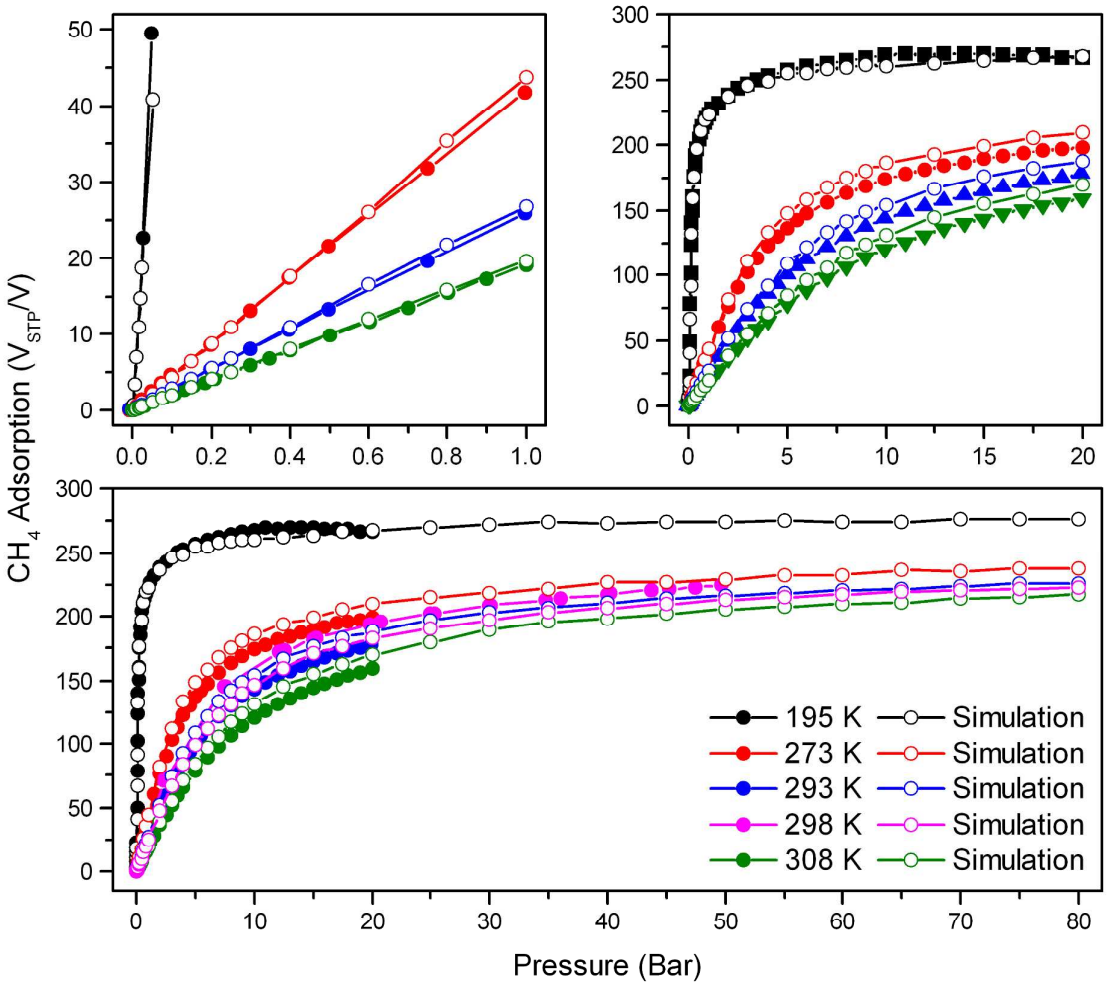

Figure S18 Comparison of the simulated and experimental adsorption isotherms for CH_4 in MFM-300(In) at 195, 273, 293 and 308 K. Excellent agreements between the experiment and simulation are observed up to 20 bar.

Positions of Adsorbed Methane Molecules as Determined by GCMC Modelling

Snapshots were taken of the Grand Canonical Monte Carlo (GCMC) modelling to gain an insight onto the packing of methane molecules within the pore of MFM-300 (In). These data allow us a qualitative insight into the filling of the porous structure of MFM-300 (In) under a variety of conditions.

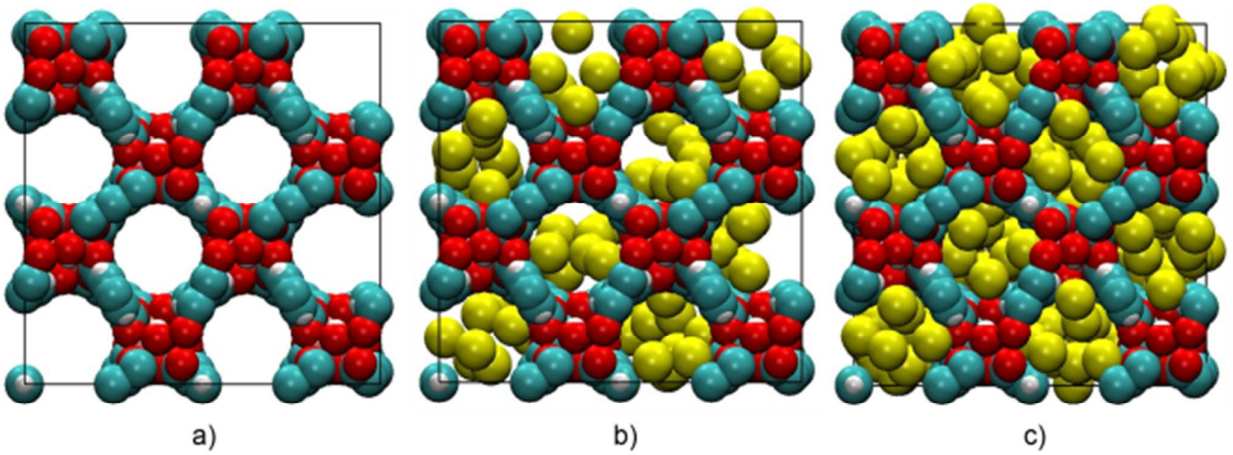

Figure S19 GCMC calculation snapshot of a) desolvated MFM-300(In); and CH_4-loaded MFM-300(In) at 195 and b) 0.1 bar and c) 80 bar.

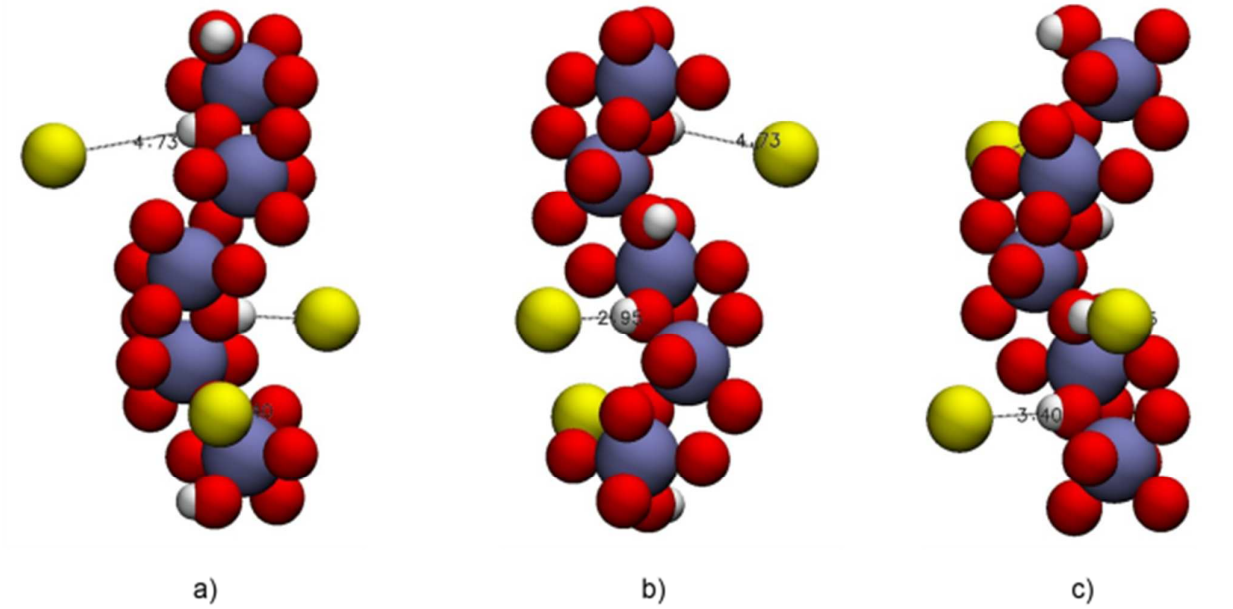

Figure S20 Views of interactions of the In-OH-In carboxylate chain with CH_4

Neutron Powder Diffraction (NPD) Experiments and Structure Determination

Neutron powder diffraction experiments were carried out at WISH, a long wavelength powder and single crystal neutron diffractometer at the ISIS Facility at the Rutherford Appleton Laboratory (UK).[6] The instrument views a solid CH_4 moderator providing a high flux of cold neutrons with a large bandwidth, transported to the sample *via* an elliptical guide. The WISH divergent jaws system allows for tuning the resolution according to the need of the experiment; in this case, it was setup in high resolution mode. The WISH detectors are 1m long, 8mm diameter pixellated 3He tubes positioned at 2.2 m from the sample and arranged on a cylindrical locus covering 10-170 degrees in 2θ scattering angle. To reduce the background from sample environment, it is equipped with an oscillating radial collimator that defines a cylinder of radius about 22 mm diameter at 90 degrees scattering.

The sample of desolvated MFM-300(In) was loaded into a cylindrical vanadium sample container with an indium vacuum seal and connected to a gas handling system. The sample was degassed at 10^{-7} mbar and 100 °C for 1 day to remove any remaining trace guest water molecules. The temperature during data collection was controlled using a helium cryostat (7 ± 0.2 K). D_2 and CD_4 were dosed at 50 and 150 K respectively to ensure that the compound of interest was present in the gas phase when not adsorbed inside the crystalline structure of MFM-300(In). The sample was dosed from a calibrated volume to 1.0, 1.5, 3.0 4.5 and 6.0 D_2 per In and 1.0, 2.0 and 3.0 CD_4 per In. The sample was then slowly cooled to 7 K to ensure the analysis gas was completely adsorbed with no condensation within the cell, sufficient time was then allowed to reach thermal equilibrium and data collected. The adsorbed gas was removed by heating the sample cell to 373 K, accompanied by returning the adsorbed gas to the dosing volume. When 95 % of the dosed gas had been returned, the sample was connected to a turbomolecular pump and degassed at 10^{-7} mbar and 373 K for two hours to ensure complete removal of the adsorbed gas.

Rietveld refinements on the NPD patterns of the bare MOF and the samples with various CD_4 loadings were performed using the TOPAS software package. The initial Fourier difference maps were used to find the isosurfaces of the three-dimensional difference scattering-length density distribution for CD_4 molecules. In this treatment the CD_4 molecules were treated as rigid bodies; we first refined the centers of mass, orientations, and

occupancies of the adsorbed CD_4, followed by full profile Rietveld refinement including the positions of metals and linkers, together with their corresponding lattice parameters, resulting in satisfactory R-factors. The final refinements on all the parameters including fractional coordinates, thermal parameters, occupancies for both host lattice and adsorbed CD_4 molecules, and background/profile coefficients yielded very good agreement factors. No restriction of the molecule position was used in the refinement. The total occupancies of CD_4 molecules obtained from the refinement are also in good agreement with the experimental values for the CD_4 loading. The refined structural parameters including the refined positions and orientations of the CD_4 rigid bodies are detailed in Table S2-S3.

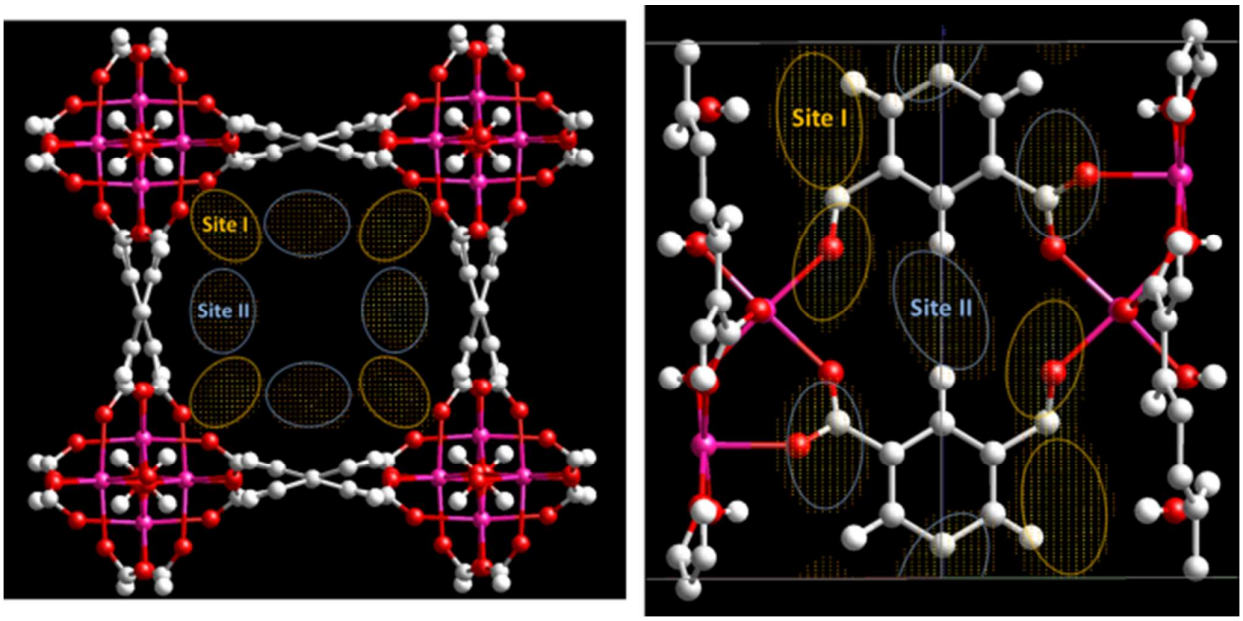

Figure S21 Fourier difference map of the residual nuclear density of MFM-300(In) at a loading of 1.09 CD_4 per In revealing the two different adsorption sites.

.

Neutron Refinement Structural Data

	MFM-300(In) Degassed	MFM-300(In) 0.90 D_2 per In	MFM-300(In) 1.60 D_2 per In	MFM-300(In) 2.99 D_2 per In	MFM-300(In) 4.83 D_2 per In	MFM-300(In) 6.08 D_2 per In
Chemical formula	$0.5(C_{16}H_8In_2O_{10})$	$0.5(C_{16}H_8In_2O_{10})$ ·(0.90 D_2)	$0.5(C_{16}H_8In_2O_{10})$ ·(1.60 D_2)	$0.5(C_{16}H_8In_2O_{10})$ ·(2.99 D_2)	$0.5(C_{16}H_8In_2O_{10})$ ·(4.83 D_2)	$0.5(C_{16}H_8In_2O_{10})$ ·(6.08 D_2)
M_r	294.93	298.59	301.38	306.95	314.37	319.39
Crystal system	Tetragonal	Tetragonal	Tetragonal	Tetragonal	Tetragonal	Tetragonal
Space group	$I4_122$	$I4_122$	$I4_122$	$I4_122$	$I4_122$	$I4_122$
Temperature	7 K	7 K	7 K	7 K	7 K	7 K
a (Å)	15.49526 (11)	15.49394 (9)	15.49227 (10)	15.48888 (13)	15.48281 (12)	15.49785 (17)
c (Å)	12.32020 (17)	12.31213 (15)	12.32047 (18)	12.30827 (19)	12.3009 (2)	12.3052 (2)
V (Å^3)	2958.12 (6)	2955.68 (5)	2954.64 (6)	2952.82 (7)	2948.74 (7)	2955.51 (8)
Z	8	8	8	8	8	8
Sample size (mm)	Cylinder, 65 x 8	Cylinder, 65 x 8	Cylinder, 65 x 8	Cylinder, 65 x 8	Cylinder, 65 x 8	Cylinder, 65 x 8
Radiation type	Neutron	Neutron	Neutron	Neutron	Neutron	Neutron
Scan method	Time of Flight	Time of Flight	Time of Flight	Time of Flight	Time of Flight	Time of Flight
R_{exp}	0.754	0.371	0.368	0.366	0.361	0.372
R_{wp}	1.426	1.256	1.430	1.530	1.684	2.026
R_p	1.686	1.354	1.408	1.467	1.479	1.597
GooF	1.891	3.388	3.388	4.180	4.666	5.451
CCDC	1043464					

Table S2 NPD structural refinement parameters of desolvated MFM-300 and at three loadings of D_2.

	MFM-300(In) Degassed	MFM-300(In) 1.09 CD_4 per In	MFM-300(In) 2.09 CD_4 per In	MFM-300(In) 3.11 CD_4 per In
Chemical formula	$0.5(C_{16}H_8In_2O_{10})$	$0.5(C_{16}H_8In_2O_{10})$ ·(1.09 CD_4)	$0.5(C_{16}H_8In_2O_{10})$ ·(2.09 CD_4)	$0.5(C_{16}H_8In_2O_{10})$ ·(3.11 CD_4)
M_r	294.93	316.73	336.82	357.21
Crystal system	Tetragonal	Tetragonal	Tetragonal	Tetragonal
Space group	$I4_122$	$I4_122$	$I4_122$	$I4_122$
Temperature	7 K	7 K	7 K	7 K
a (Å)	15.49526 (11)	15.46363 (5)	15.43745 (10)	15.5019 (3)
c (Å)	12.32020 (17)	12.29044 (10)	12.2848 (2)	12.3060 (3)
V (Å^3)	2958.12 (6)	2938.94 (3)	2927.65 (6)	2957.24 (14)
Z	8	8	8	8
Sample size (mm)	Cylinder, 65 x 8	Cylinder, 65 x 8	Cylinder, 65 x 8	Cylinder, 65 x 8
Radiation type	Neutron	Neutron	Neutron	Neutron
Scan method	Time of Flight	Time of Flight	Time of Flight	Time of Flight
R_{exp}	0.754	0.826	0.317	0.308
R_{wp}	1.426	1.560	1.624	1.688
R_p	1.686	1.217	1.499	1.625
GooF	1.891	1.889	5.115	5.472
CCDC	1043464	1043465	1043466	1043467

Table S3 NPD structural refinement parameters of desolvated MFM-300 and at three loadings of CD_4.

Tables of Atomic Parameters for Desolvated, D_2 and CD_4 Loaded MFM-300(In)

0.5($C_{16}H_8In_2O_{10}$)

	m	*x*	*Y*	z	U_{iso}
In	8	0.6859(2)	0.3141(2)	0.5	0.040(2)
O1	8	0.7573(2)	0.25	0.625	0.0484(9)
O2	16	0.6126(4)	0.3828(4)	0.6166(3)	0.0484(9)
O3	16	0.5939(4)	0.2931(3)	0.7540(4)	0.0484(9)
C1	16	0.5849(3)	0.3642(2)	0.7084(2)	0.0431(6)
C2	16	0.53782(10)	0.43117(8)	0.7675(2)	0.0431(6)
C3	8	0.5	0.5	0.7105(3)	0.0431(6)
C4	16	0.53782(10)	0.43117(8)	0.88155(15)	0.0431(6)
C5	8	0.5	0.5	0.93859(14)	0.0431(6)
H1	8	0.8154(5)	0.25	0.625	0.0484(9)
H3	8	0.5	0.5	0.6252(4)	0.0431(6)
H4	16	0.5661(2)	0.3797(2)	0.9242(2)	0.0431(6)

Table S4 Atomic positions and isotropic displacement parameters for desolvated MFM-300(In).

0.5($C_{16}H_8In_2O_{10}$)·(0.90 D_2)

	m	*x*	*Y*	*z*	U_{iso}	Occ. (<1)
In	8	0.6867 (2)	0.3133 (2)	0.5	0.036 (2)	
O1	8	0.7576 (2)	0.25	0.625	0.0466 (8)	
O2	16	0.6119 (4)	0.3812 (4)	0.6165 (3)	0.0466 (8)	
O3	16	0.5938 (4)	0.2924 (3)	0.7534 (3)	0.0466 (8)	
C1	16	0.5840 (3)	0.3638 (2)	0.7087 (2)	0.0419 (6)	
C2	16	0.53713 (11)	0.43092 (8)	0.76779 (19)	0.0419 (6)	
C3	8	0.5	0.5	0.7108 (2)	0.0419 (6)	
C4	16	0.53713 (11)	0.43092 (8)	0.88175 (13)	0.0419 (6)	
C5	8	0.5	0.5	0.93874 (13)	0.0419 (6)	
H1	8	0.8157 (5)	0.25	0.625	0.0466 (8)	
H3	8	0.5	0.5	0.6255 (4)	0.0419 (6)	
H4	16	0.5649 (2)	0.3792 (2)	0.9244 (2)	0.0419 (6)	
D2_1	16	0.4770 (3)	0.7462 (9)	0.1619 (6)	0.210 (5)	0.736 (5)
D2_2	8	0.6579 (12)	0.6579 (12)	0.5	0.38 (3)	0.346 (18)

Table S5 Atomic positions and isotropic displacement parameters for MFM-300(In) at a loading of 0.90 D_2 molecules per In

0.5($C_{16}H_8In_2O_{10}$)·(1.60 D_2)

	m	*x*	*Y*	*z*	U_{iso}	Occ. (<1)
In	8	0.6840 (3)	0.3160 (3)	0.5	0.042 (3)	
O1	8	0.7604 (3)	0.25000	0.62500	0.0507 (10)	
O2	16	0.6125 (5)	0.3822 (5)	0.6158 (3)	0.0507 (10)	
O3	16	0.5926 (5)	0.2918 (3)	0.7540 (4)	0.0507 (10)	
C1	16	0.5836 (3)	0.3644 (3)	0.7090 (2)	0.0407 (6)	
C2	16	0.53747 (13)	0.43122 (9)	0.7676 (2)	0.0407 (6)	
C3	8	0.5	0.5	0.7107 (3)	0.0407 (6)	
C4	16	0.53747 (13)	0.43122 (9)	0.88142 (15)	0.0407 (6)	
C5	8	0.5	0.5	0.93833 (14)	0.0407 (6)	
H1	8	0.8185 (6)	0.25	0.62500	0.0507 (10)	
H3	8	0.5	0.5	0.6254 (5)	0.0407 (6)	
H4	16	0.5655 (3)	0.3797 (3)	0.9241 (2)	0.0407 (6)	
D2_1	16	0.4777 (3)	0.7505 (8)	0.1702 (5)	0.238 (5)	0.915 (6)
D2_2	8	0.6314 (5)	0.6314 (5)	0.5	0.380 (14)	0.99 (2)
D2_3	8	0.75	0.9157 (13)	0.875	0.210 (18)	0.386 (14)

Table S6 Atomic positions and isotropic displacement parameters for MFM-300(In) at a loading of 1.60 D_2 molecules per In

0.5($C_{16}H_8In_2O_{10}$)·(2.99 D_2)

	m	*x*	*Y*	*z*	U_{iso}	Occ. (<1)
In	8	0.6842 (3)	0.3158 (3)	0.5	0.036 (3)	
O1	8	0.7608 (3)	0.25	0.625	0.0514 (11)	
O2	16	0.6118 (5)	0.3797 (5)	0.6166 (4)	0.0514 (11)	
O3	16	0.5924 (5)	0.2934 (3)	0.7531 (5)	0.0514 (11)	
C1	16	0.5846 (4)	0.3642 (3)	0.7087 (3)	0.0376 (8)	
C2	16	0.54133 (14)	0.43280 (12)	0.7676 (3)	0.0376 (8)	
C3	8	0.5	0.50000	0.7103 (3)	0.0376 (8)	
C4	16	0.54133 (14)	0.43280 (12)	0.8823 (2)	0.0376 (8)	
C5	8	0.5	0.5	0.93958 (19)	0.0376 (8)	
H1	8	0.8189 (7)	0.25	0.625	0.0514 (11)	
H3	8	0.5	0.5	0.6250 (6)	0.0376 (8)	
H4	16	0.5721 (3)	0.3828 (3)	0.9249 (3)	0.0376 (8)	
D2_1	16	0.4704 (4)	0.7560 (6)	0.1852 (6)	0.176 (5)	0.920 (10)
D2_2	8	0.6186 (5)	0.6186 (5)	0.5	0.380 (11)	1.44 (2)
D2_3	8	0.75	0.9057 (9)	0.875	0.367 (15)	1.09 (3)
D2_4	16	0.7350 (7)	0.5640 (6)	0.7024 (10)	0.277 (10)	0.804 (17)

Table S7 Atomic positions and isotropic displacement parameters for MFM-300(In) at a loading of 2.99 D_2 molecules per In

0.5($C_{16}H_8In_2O_{10}$)·(4.83 D_2)

	m	*x*	*Y*	*z*	U_{iso}	Occ. (<1)
In	8	0.6833 (4)	0.3167 (4)	0.5	0.028 (3)	
O1	8	0.7549 (5)	0.25	0.625	0.0502 (13)	
O2	16	0.6115 (6)	0.3793 (6)	0.6153 (5)	0.0502 (13)	
O3	16	0.5933 (6)	0.2922 (4)	0.7550 (6)	0.0502 (13)	
C1	16	0.5848 (5)	0.3637 (3)	0.7092 (4)	0.0322 (9)	
C2	16	0.54161 (17)	0.43240 (14)	0.7681 (3)	0.0322 (9)	
C3	8	0.5	0.5	0.7104 (4)	0.0322 (9)	
C4	16	0.54161 (17)	0.43240 (14)	0.8835 (2)	0.0322 (9)	
C5	8	0.5	0.5	0.9412 (2)	0.0322 (9)	
H1	8	0.8130 (10)	0.25	0.625	0.0502 (13)	
H3	8	0.5	0.5	0.6273 (6)	0.0322 (9)	
H4	16	0.5716 (3)	0.3837 (3)	0.9250 (3)	0.0322 (9)	
D2_1	16	0.4652 (5)	0.7581 (5)	0.1962 (6)	0.222 (6)	1.230 (15)
D2_2	8	0.6173 (8)	0.6173 (8)	0.5	0.380 (19)	1.00 (3)
D2_3	8	0.75	0.9103 (8)	0.875	0.313 (13)	1.52 (3)
D2_4	16	0.7228 (8)	0.5569 (8)	0.6794 (10)	0.262 (10)	1.23 (3)
D2_5	16	0.6743 (12)	0.8598 (15)	0.1771 (10)	0.314 (15)	0.755 (18)
D2_6	16	0.7017 (14)	0.5759 (14)	0.814 (2)	0.142 (14)	0.36 (2)

Table S8 Atomic positions and isotropic displacement parameters for MFM-300(In) at a loading of 4.83 D_2 molecules per In

0.5($C_{16}H_8In_2O_{10}$)·(6.08 D_2)

	m	*x*	*Y*	*z*	U_{iso}	Occ. (<1)
In	8	0.6805 (5)	0.3195 (5)	0.5	0.022 (4)	
O1	8	0.7557 (6)	0.25000	0.625	0.0612 (19)	
O2	16	0.6082 (8)	0.3773 (8)	0.6167 (6)	0.0612 (19)	
O3	16	0.5918 (9)	0.2924 (5)	0.7553 (8)	0.0612 (19)	
C1	16	0.5828 (6)	0.3626 (4)	0.7098 (5)	0.0332 (10)	
C2	16	0.5400 (2)	0.43149 (18)	0.7687 (4)	0.0332 (10)	
C3	8	0.5	0.5	0.7110 (5)	0.0332 (10)	
C4	16	0.5400 (2)	0.43149 (18)	0.8841 (3)	0.0332 (10)	
C5	8	0.5	0.5	0.9418 (3)	0.0332 (10)	
H1	8	0.8138 (12)	0.25	0.625	0.0612 (19)	
H3	8	0.5	0.5	0.6299 (8)	0.0332 (10)	
H4	16	0.5681 (4)	0.3833 (5)	0.9246 (4)	0.0332 (10)	
D2_1	16	0.4589 (5)	0.7586 (7)	0.2017 (8)	0.210 (6)	1.274 (19)
D2_2	8	0.6118 (8)	0.6118 (8)	0.5	0.380 (19)	1.24 (3)
D2_3	8	0.75	0.9163 (12)	0.875	0.346 (14)	2.00 (6)
D2_4	16	0.7211 (7)	0.5477 (6)	0.6946 (9)	0.252 (10)	1.40 (3)
D2_5	16	0.6829 (11)	0.8685 (12)	0.1532 (12)	0.284 (14)	1.09 (3)
D2_6	16	0.6778 (10)	0.6174 (9)	0.8286 (14)	0.074 (10)	0.45 (2)
D2_7	16	0.681 (7)	0.693 (6)	0.699 (6)	0.380 (19)	0.25 (2)

Table S9 Atomic positions and isotropic displacement parameters for MFM-300(In) at a loading of 6.08 D_2 molecules per In

0.5($C_{16}H_8In_2O_{10}$)·(1.09 CD_4)

	m	*x*	*Y*	*z*	U_{iso}	Occ. (<1)
In	8	0.6875(4)	0.3125(4)	0.5	0.085(5)	
O1	8	0.7617(3)	0.25	0.625	0.075(2)	
O2	16	0.6139(6)	0.3806(7)	0.6160(4)	0.075(2)	
O3	16	0.5938(7)	0.2910(4)	0.7512(5)	0.075(2)	
C1	16	0.5837(5)	0.3644(4)	0.7088(3)	0.0779(14)	
C2	16	0.53685(17)	0.43088(11)	0.7674(2)	0.0779(14)	
C3	8	0.5	0.5	0.7106(3)	0.0779(14)	
C4	16	0.53685(17)	0.43088(11)	0.88125(16)	0.0779(14)	
C5	8	0.5	0.5	0.93814(15)	0.0779(14)	
H1	8	0.8199(8)	0.25	0.625	0.075(2)	
H3	8	0.5	0.5	0.6251(6)	0.0779(14)	
H4	16	0.5645(4)	0.3790(4)	0.9240(3)	0.0779(14)	
C1_1	16	0.5127(2)	0.7333(8)	0.1360(7)	0.190(6)	0.398(2)
D1_1	16	0.552(3)	0.783(2)	0.1642(15)	0.228(9)	0.398(2)
D2_1	16	0.5034(8)	0.7402(15)	0.0522(10)	0.228(9)	0.398(2)
D3_1	16	0.4530(8)	0.736(3)	0.1756(14)	0.228(9)	0.398(2)
D4_1	16	0.542(3)	0.6737(19)	0.1519(15)	0.228(9)	0.398(2)
C1_2	8	0.6399(5)	0.6399(5)	0.5	0.190(6)	0.292(6)
D1_2	16	0.663(3)	0.649(4)	0.578(2)	0.228(9)	0.146(2)
D4_2	16	0.648(2)	0.696(2)	0.456(4)	0.228(9)	0.146(2)
D2_2	16	0.5753(16)	0.624(2)	0.503(4)	0.228(9)	0.146(2)
D3_2	16	0.674(3)	0.5906(18)	0.464(4)	0.228(9)	0.146(2)

Table S10 Atomic positions and isotropic displacement parameters for MFM-300(In) at a loading of 1.09 CD_4 molecules per In.

0.5($C_{16}H_8In_2O_{10}$)·(2.09 CD_4)

	m	*x*	*Y*	*z*	U_{iso}	Occ. (<1)
In	8	0.6837(4)	0.3163(4)	0.5	0.058(3)	
O1	8	0.7580(4)	0.25	0.625	0.0602(13)	
O2	16	0.6140(6)	0.3806(7)	0.6173(5)	0.0602(13)	
O3	16	0.5910(7)	0.2909(4)	0.7508(6)	0.0602(13)	
C1	16	0.5833(5)	0.3637(4)	0.7085(4)	0.0578(9)	
C2	16	0.53734(17)	0.43096(13)	0.7673(3)	0.0578(9)	
C3	8	0.5	0.5	0.7104(4)	0.0578(9)	
C4	16	0.53734(17)	0.43096(13)	0.8812(2)	0.0578(9)	
C5	8	0.5	0.5	0.9381(2)	0.0578(9)	
H1	8	0.8163(8)	0.25	0.625	0.0602(13)	
H3	8	0.5	0.5	0.6249(7)	0.0578(9)	
H4	16	0.5654(4)	0.3792(4)	0.9239(4)	0.0578(9)	
C1_1	16	0.5197(3)	0.7430(5)	0.1781(4)	0.129(4)	0.463(4)
D1_1	16	0.5306(8)	0.7466(9)	0.2607(6)	0.155(4)	0.463(4)
D2_1	16	0.5567(8)	0.7890(8)	0.1390(10)	0.155(4)	0.463(4)
D3_1	16	0.4552(5)	0.7542(10)	0.1624(10)	0.155(4)	0.463(4)
D4_1	16	0.5365(9)	0.6823(7)	0.1505(10)	0.155(4)	0.463(4)
C1_2	8	0.6349(3)	0.6349(3)	0.5	0.129(4)	0.596(6)
D1_2	16	0.640(2)	0.5775(8)	0.5421(14)	0.155(4)	0.298(3)
D2_2	16	0.5704(8)	0.650(3)	0.4892(17)	0.155(4)	0.298(3)
D3_2	16	0.6644(13)	0.6287(16)	0.4252(10)	0.155(4)	0.298(3)
D4_2	16	0.665(2)	0.6836(14)	0.5435(14)	0.155(4)	0.298(3)
C1_3	16	0.6078(5)	0.7379(5)	0.3633(7)	0.129(4)	0.284(4)
D1_3	16	0.642(2)	0.6844(17)	0.3368(17)	0.155(4)	0.284(4)
D2_3	16	0.6402(15)	0.7659(13)	0.4275(14)	0.155(4)	0.284(4)
D3_3	16	0.5469(12)	0.719(3)	0.3881(17)	0.155(4)	0.284(4)
D4_3	16	0.603(2)	0.7819(12)	0.3006(15)	0.155(4)	0.284(4)

Table S11 Atomic positions and isotropic displacement parameters for MFM-300(In) at a loading of 2.09 CD_4 molecules per In.

0.5($C_{16}H_8In_2O_{10}$)·(3.11 CD_4)

	m	*x*	*y*	*z*	U_{iso}	Occ. (<1)
In	8	0.6719(8)	0.3281(8)	0.5	0.139(8)	
O1	8	0.7575(6)	0.25	0.625	0.085(2)	
O2	16	0.6135(9)	0.3817(9)	0.6182(6)	0.085(2)	
O3	16	0.5881(10)	0.2912(6)	0.7545(8)	0.085(2)	
C1	16	0.5829(7)	0.3643(5)	0.7104(5)	0.0561(11)	
C2	16	0.5391(2)	0.43248(18)	0.7693(4)	0.0561(11)	
C3	8	0.5	0.5	0.7126(5)	0.0561(11)	
C4	16	0.5391(2)	0.43248(18)	0.8828(3)	0.0561(11)	
C5	8	0.5	0.5	0.9395(2)	0.0561(11)	
H1	8	0.8155(13)	0.25	0.625	0.085(2)	
H3	8	0.5	0.5	0.6273(10)	0.0561(11)	
H4	16	0.5684(5)	0.3817(6)	0.9254(5)	0.0561(11)	
C1_1	16	0.5148(7)	0.7382(6)	0.2037(6)	0.179(5)	0.504(6)
D1_1	16	0.5496(14)	0.7939(11)	0.185(2)	0.214(5)	0.504(6)
D2_1	16	0.4492(9)	0.7491(14)	0.1898(16)	0.214(5)	0.504(6)
D3_1	16	0.5244(14)	0.7224(15)	0.2853(10)	0.214(5)	0.504(6)
D4_1	16	0.5359(15)	0.6874(13)	0.1547(15)	0.214(5)	0.504(6)
C1_2	8	0.6389(5)	0.6389(5)	0.5	0.179(5)	0.582(10)
D1_2	16	0.634(9)	0.5779(19)	0.536(3)	0.214(5)	0.291(4)
D2_2	16	0.619(3)	0.635(3)	0.4189(16)	0.214(5)	0.291(4)
D3_2	16	0.703(3)	0.660(9)	0.504(3)	0.214(5)	0.291(4)
D4_2	16	0.599(5)	0.682(6)	0.542(4)	0.214(5)	0.291(4)
C1_3	16	0.6239(6)	0.7689(6)	0.3117(8)	0.179(5)	0.478(6)
D1_3	16	0.6103(14)	0.7912(13)	0.3894(13)	0.214(5)	0.478(6)
D2_3	16	0.5678(11)	0.7453(14)	0.2764(17)	0.214(5)	0.478(6)
D3_3	16	0.6695(13)	0.7200(12)	0.3161(17)	0.214(5)	0.478(6)
D4_3	16	0.6479(14)	0.8193(12)	0.2650(16)	0.214(5)	0.478(6)
C1_4	8	0.75	0.8979(9)	0.875	0.179(5)	0.564(14)
D1_4	16	0.710(5)	0.937(5)	0.830(4)	0.214(5)	0.282(6)
D2_4	16	0.778(4)	0.934(5)	0.936(5)	0.214(5)	0.282(6)
D3_4	16	0.798(3)	0.873(6)	0.826(3)	0.214(5)	0.282(6)
D4_4	16	0.715(6)	0.848(4)	0.908(6)	0.214(5)	0.282(6)

Table S12 Atomic positions and isotropic displacement parameters for MFM-300(In) at a loading of 3.11 CD_4 molecules per In.

Refined Neutron Profiles

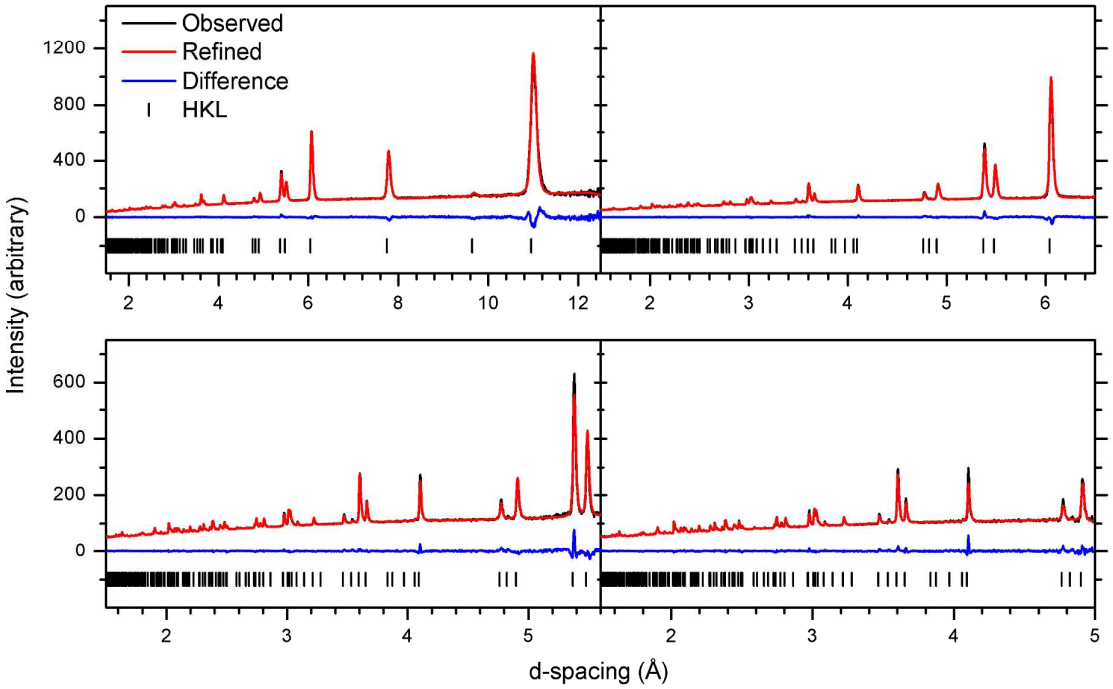

Figure S22 Observed (black), calculated (red) and difference (blue) neutron powder diffraction profiles of four of the detector banks of the WISH diffractometer for activated MFM-300(In). Each bank has a different resolution. The refinement was carried out by combining all four banks of detectors.

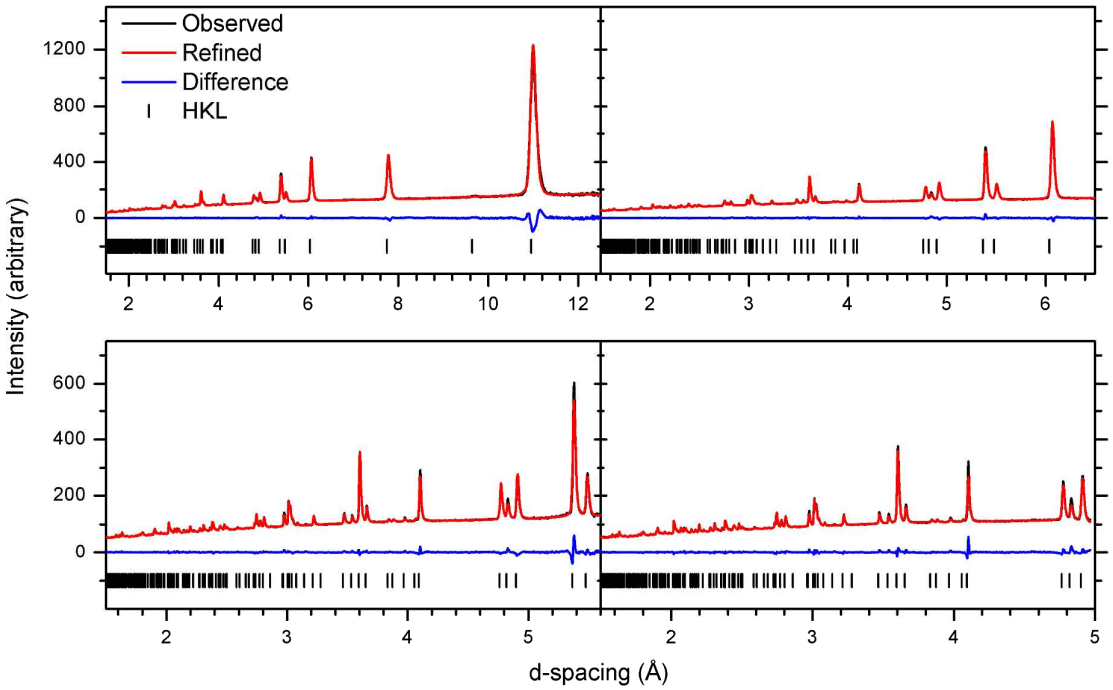

Figure S23 Observed (black), calculated (red) and difference (blue) neutron powder diffraction profiles of four of the detector banks of the WISH diffractometer for MFM-300(In) with a loading of 0.90 D_2 molecules per In. Each bank has a different resolution. The refinement was carried out by combining all four banks of detectors.

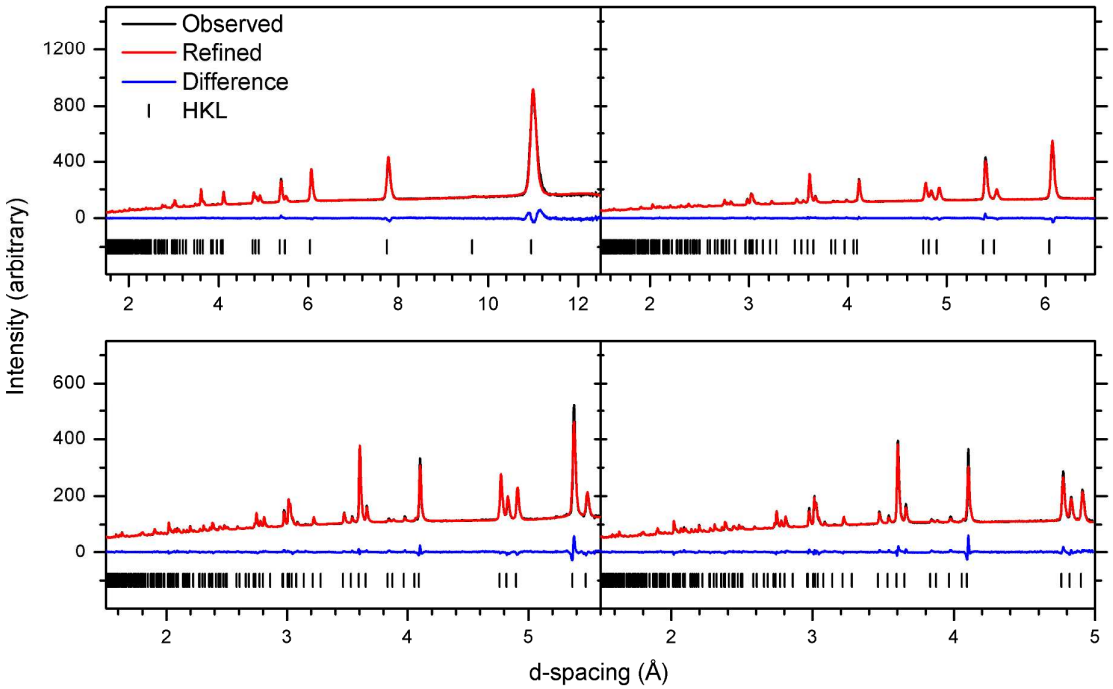

Figure S24 Observed (black), calculated (red) and difference (blue) neutron powder diffraction profiles of four of the detector banks of the WISH diffractometer for MFM-300(In) with a loading of 1.60 D_2 molecules per In. Each bank has a different resolution. The refinement was carried out by combining all four banks of detectors.

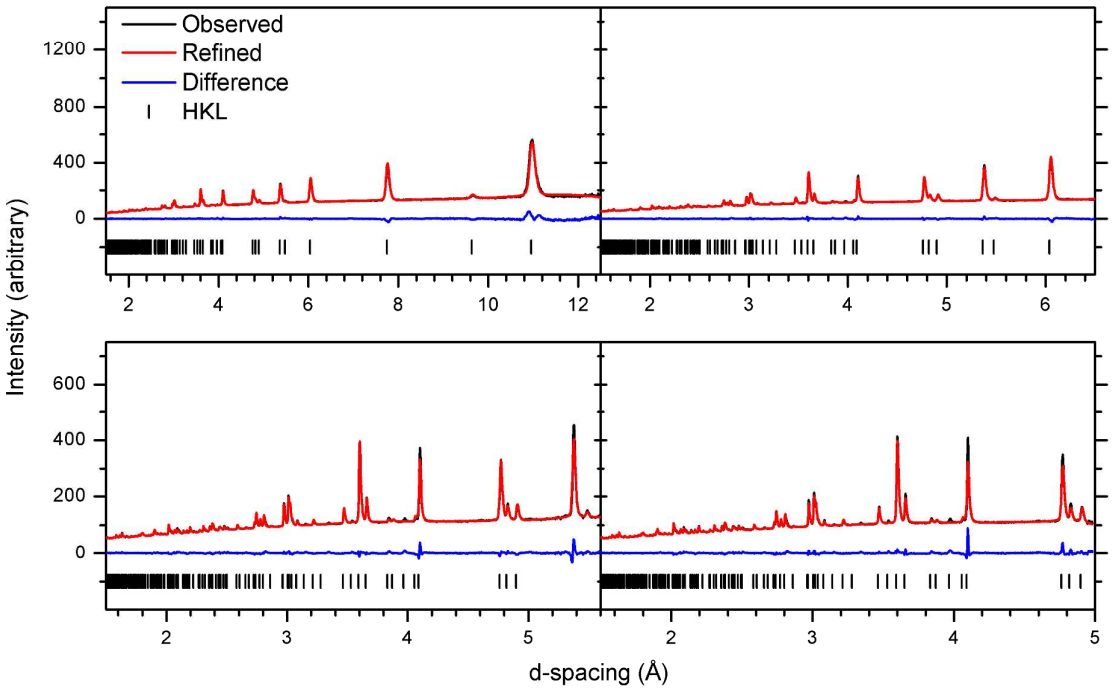

Figure S25 Observed (black), calculated (red) and difference (blue) neutron powder diffraction profiles of four of the detector banks of the WISH diffractometer for MFM-300(In) with a loading of 2.99 D_2 molecules per In. Each bank has a different resolution. The refinement was carried out by combining all four banks of detectors.

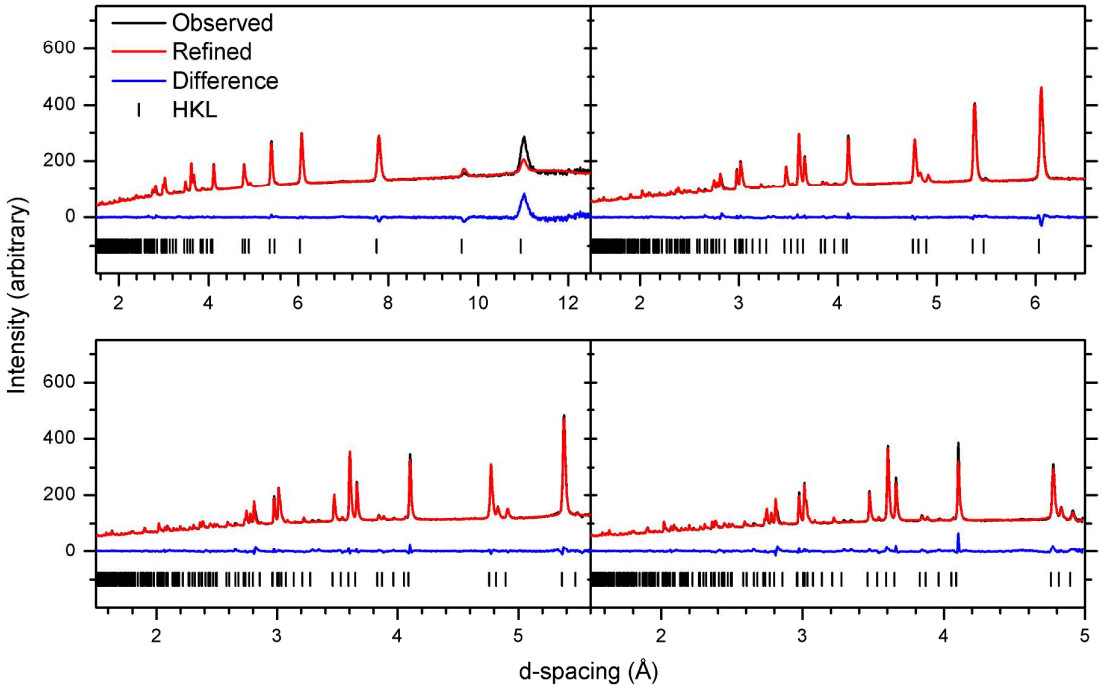

Figure S26 Observed (black), calculated (red) and difference (blue) neutron powder diffraction profiles of four of the detector banks of the WISH diffractometer for MFM-300(In) with a loading of 4.83 D_2 molecules per In. Each bank has a different resolution. The refinement was carried out by combining all four banks of detectors.

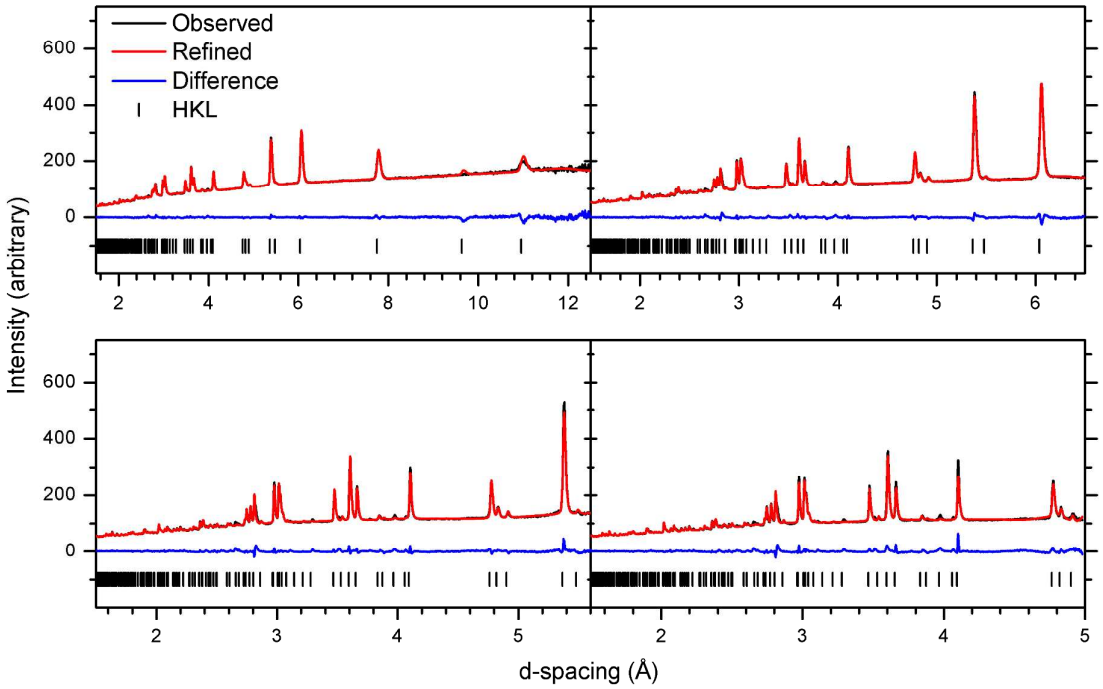

Figure S27 Observed (black), calculated (red) and difference (blue) neutron powder diffraction profiles of four of the detector banks of the WISH diffractometer for MFM-300(In) with a loading of 6.08 D_2 molecules per In. Each bank has a different resolution. The refinement was carried out by combining all four banks of detectors.

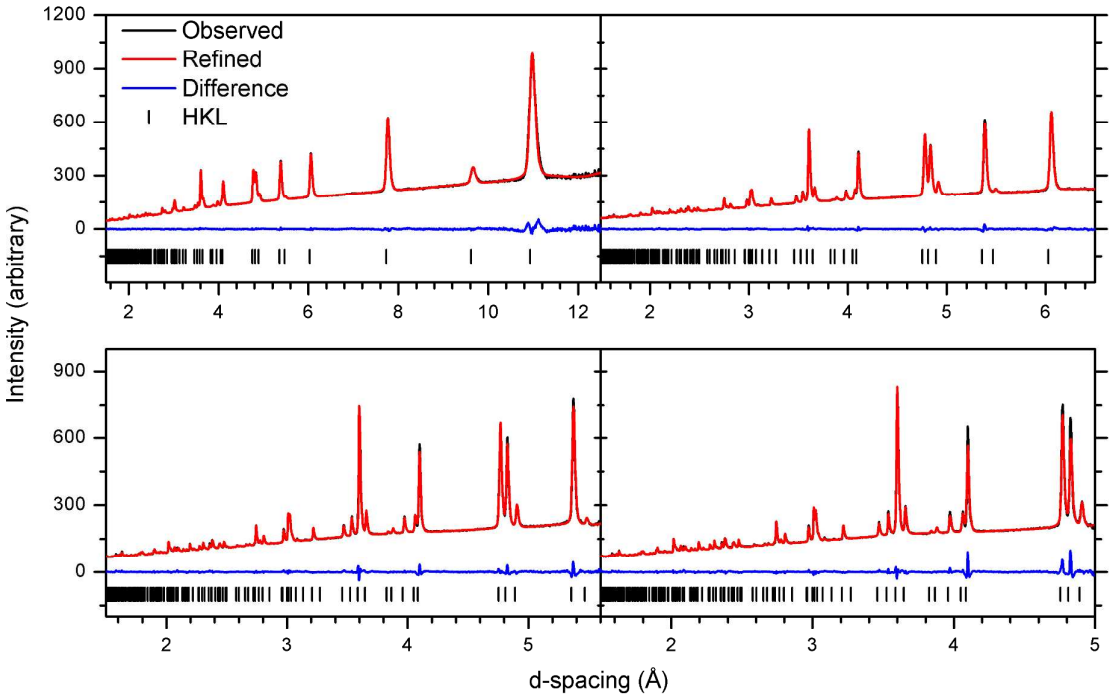

Figure S28 Observed (black), calculated (red) and difference (blue) neutron powder diffraction profiles of four of the detector banks of the WISH diffractometer for MFM-300(In) with a loading of 1.09 CD_4 molecules per In. Each bank has a different resolution. The refinement was carried out by combining all four banks of detectors.

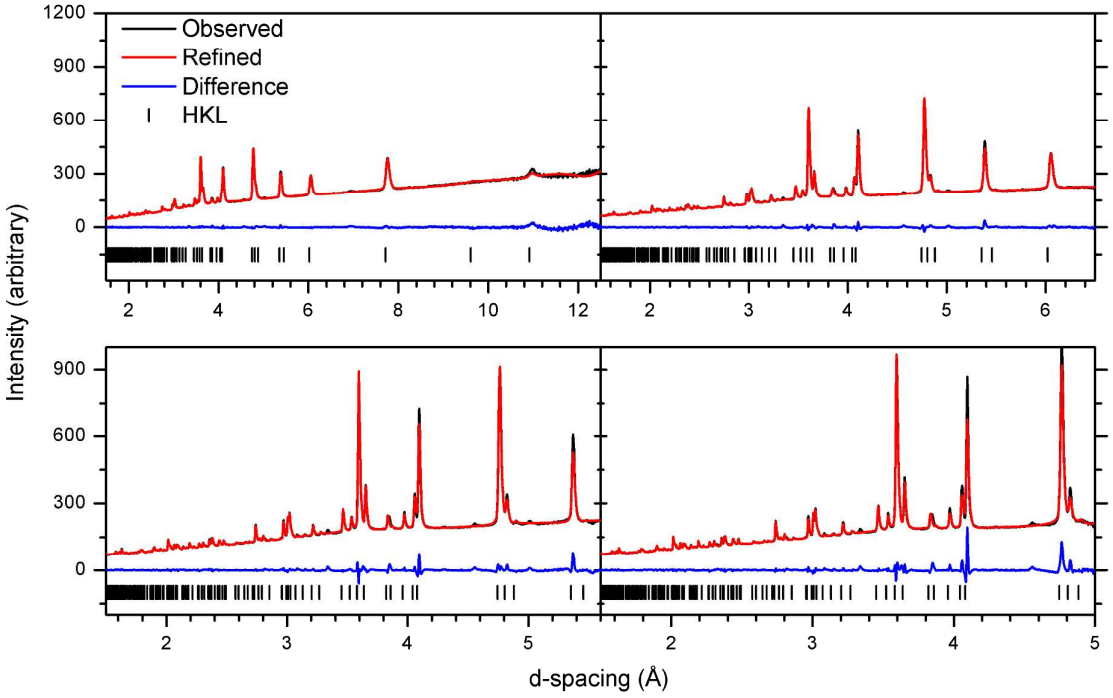

Figure S29 Observed (black), calculated (red) and difference (blue) neutron powder diffraction profiles of four of the detector banks of the WISH diffractometer for MFM-300(In) with a loading of 2.09 CD_4 molecules per In. Each bank has a different resolution. The refinement was carried out by combining all four banks of detectors.

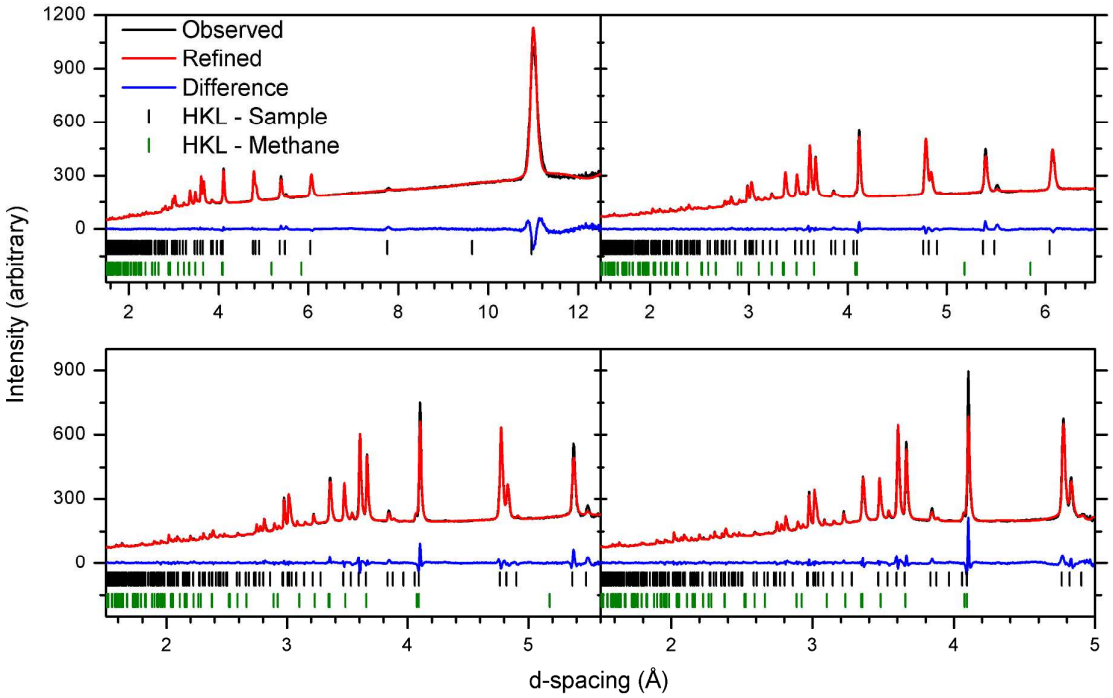

Figure S30 Observed (black), calculated (red) and difference (blue) neutron powder diffraction profiles of four of the detector banks of the WISH diffractometer for MFM-300(In) with a loading of 3.11 CD_4 molecules per In. A small amount of condensed methane (3.42%) is present at this saturated loading according to the refinement.

Fourier Difference Map

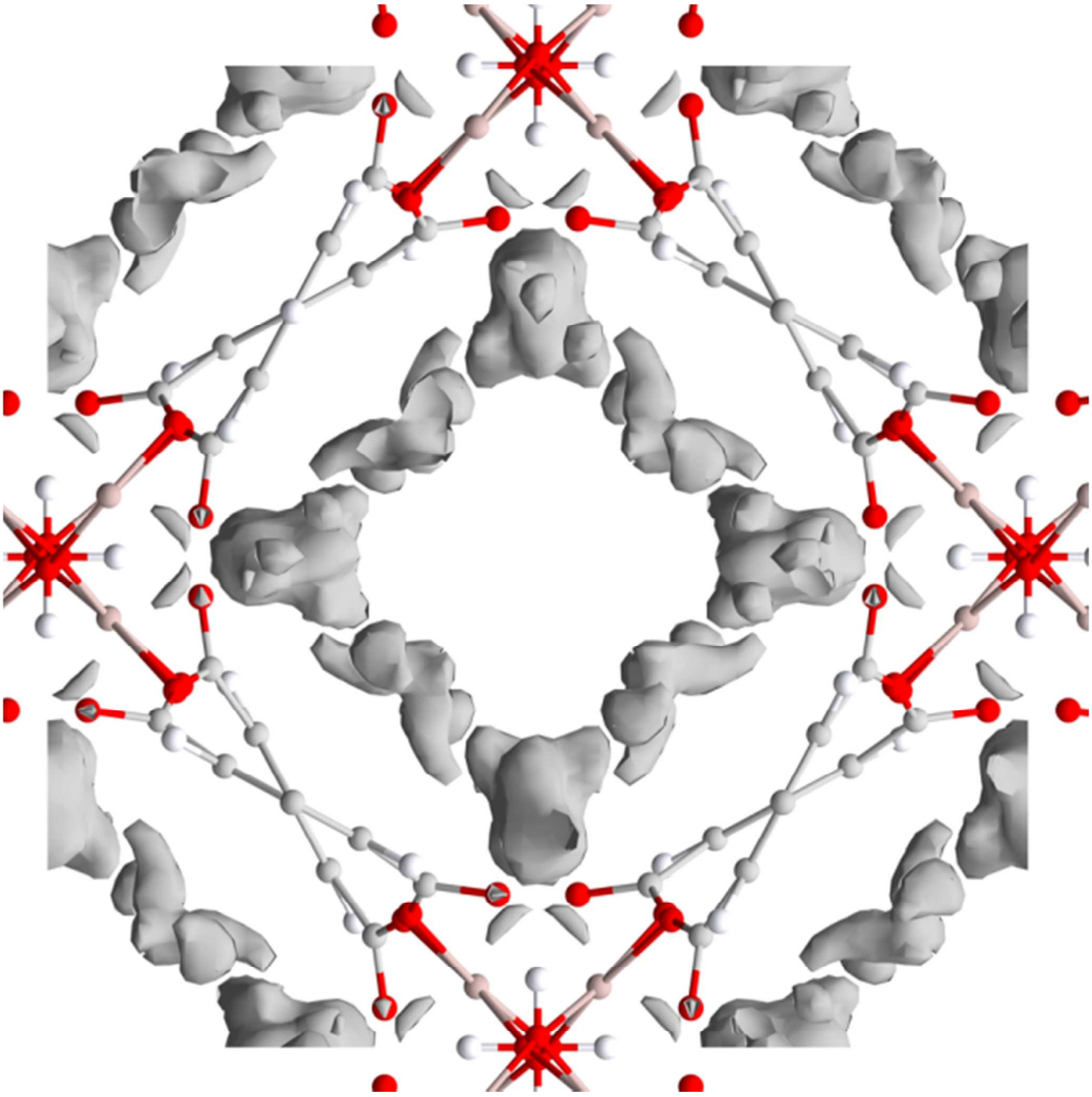

Figure S31 Fourier difference map of the residual nuclear density of MFM-300(In) at a loading of 1.09 CD_4 per In revealing the two different adsorption sites.

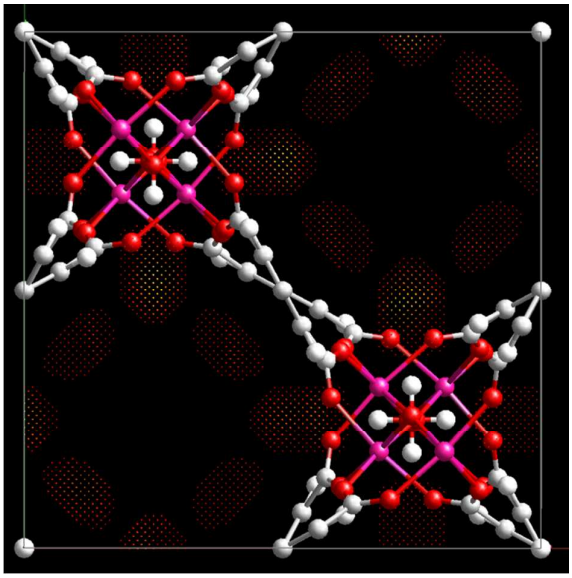

Figure S32 Fourier difference map of the residual nuclear density peaks of MFM-300(In) at a loading of 0.90 D_2 per In revealing the two different adsorption sites.

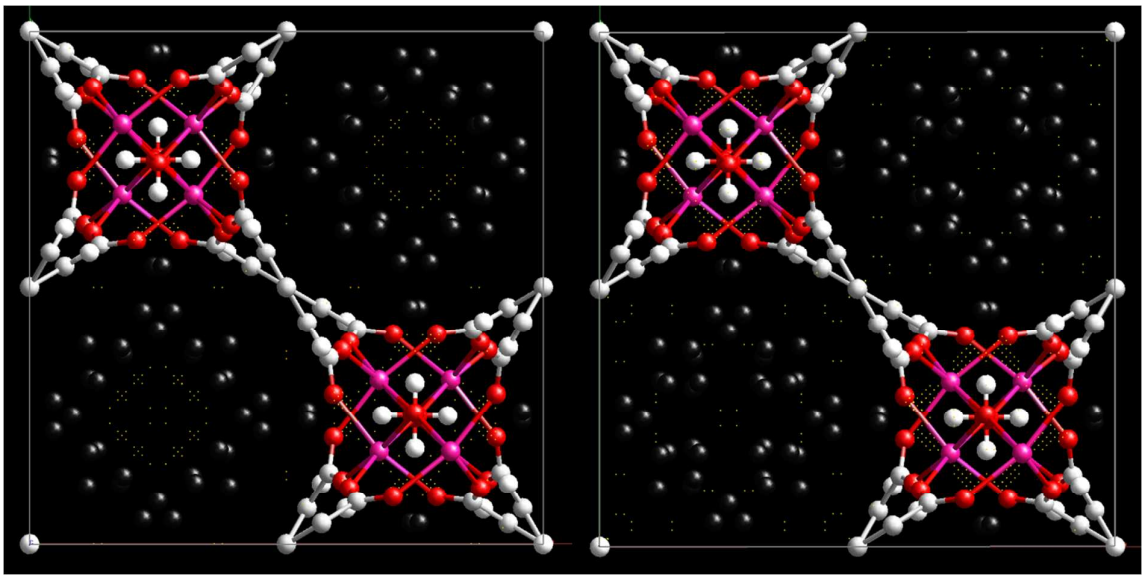

a b

Figure S33 Comparison of the Fourier difference maps of the residual nuclear density of MFM-300(In) at a loading of 6.08D_2 per In (a) without Site VII in the model and (b) with Site VII in the model. Clear residual density peaks were seen in (a), demonstrating the significance of including the additional binding site VII. In contrast, no significant residual density peak was found in (b), indicating the satisfactory refinement model by including all the significant binding sites.

Additional Crystal Structure Views of the Gas Loaded Material

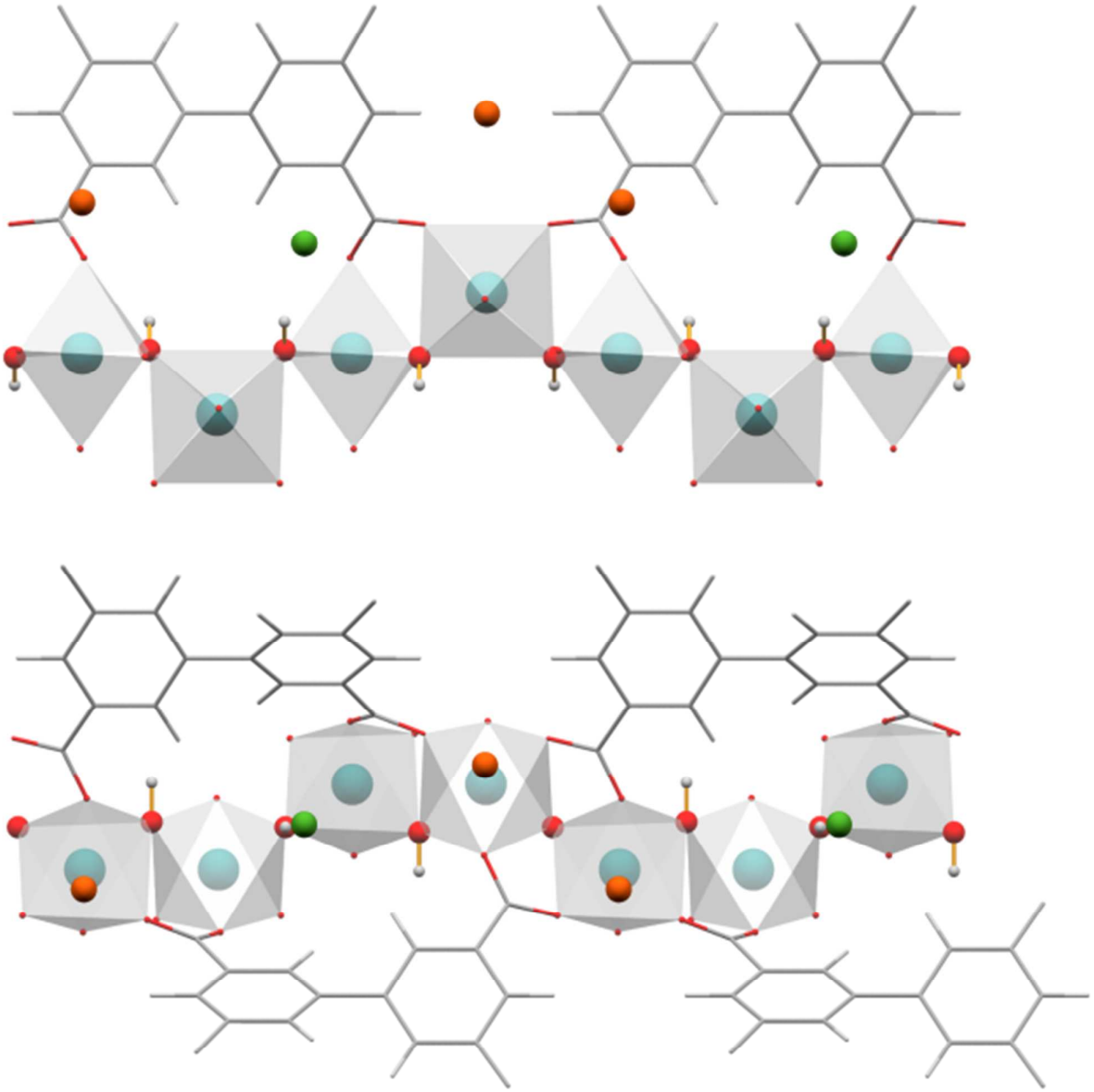

Figure S34 Two views of the *c* crystallographic axis of MFM-300(In) at a gas loading of 0.90 D_2 per In ($[In_2(OH)_2(C_{16}H_6O_8)]\cdot 1.80\ D_2$), highlighting the CD_4 binding sites (Site I, green; Site II, orange).

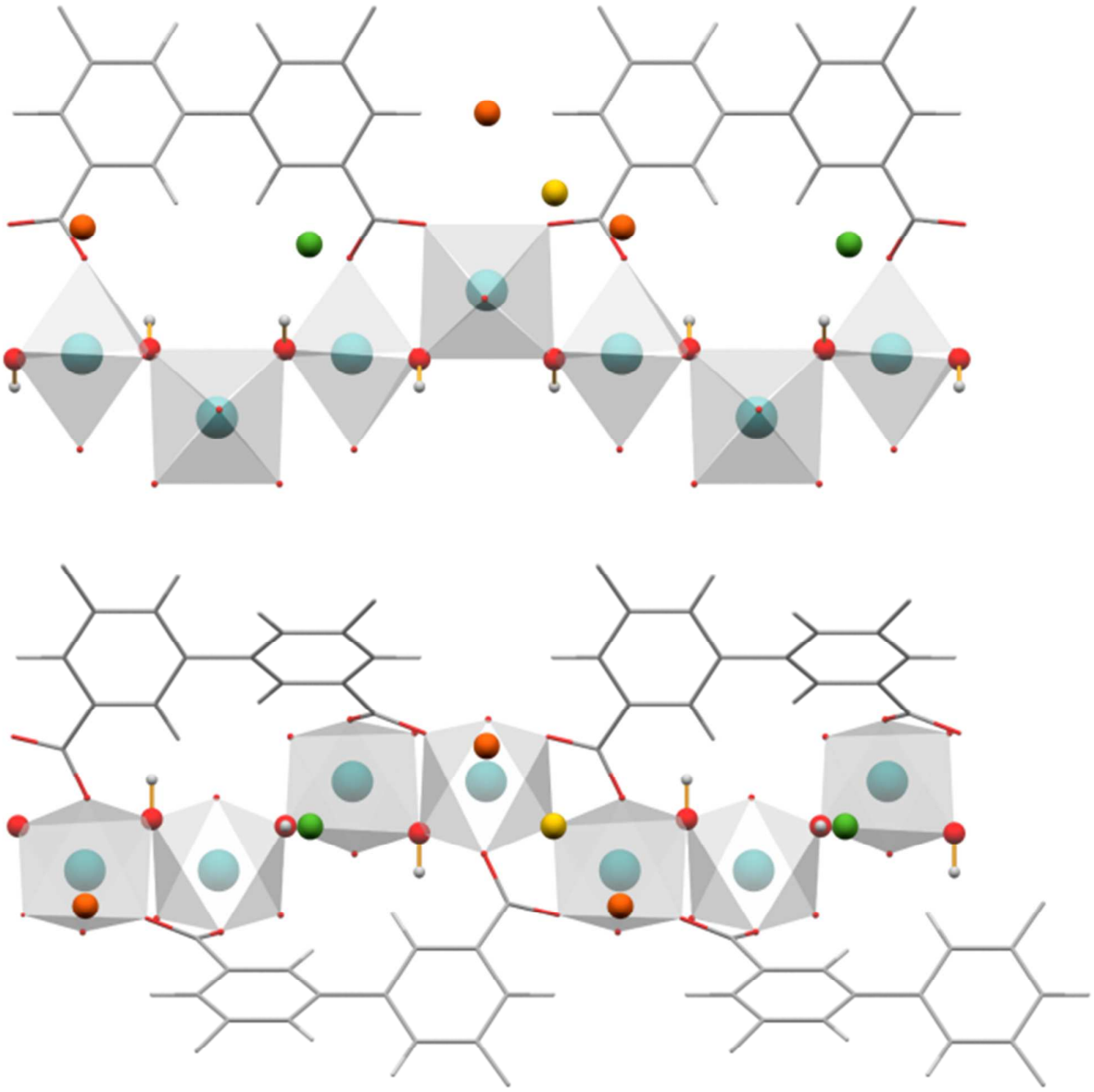

Figure S35 Two views of the *c* crystallographic axis of MFM-300(In) at a gas loading of 1.60 D_2 per In ($[In_2(OH)_2(C_{16}H_6O_8)]\cdot 3.20\ D_2$), highlighting the CD_4 binding sites (Site I, green; Site II, orange; Site III, yellow).

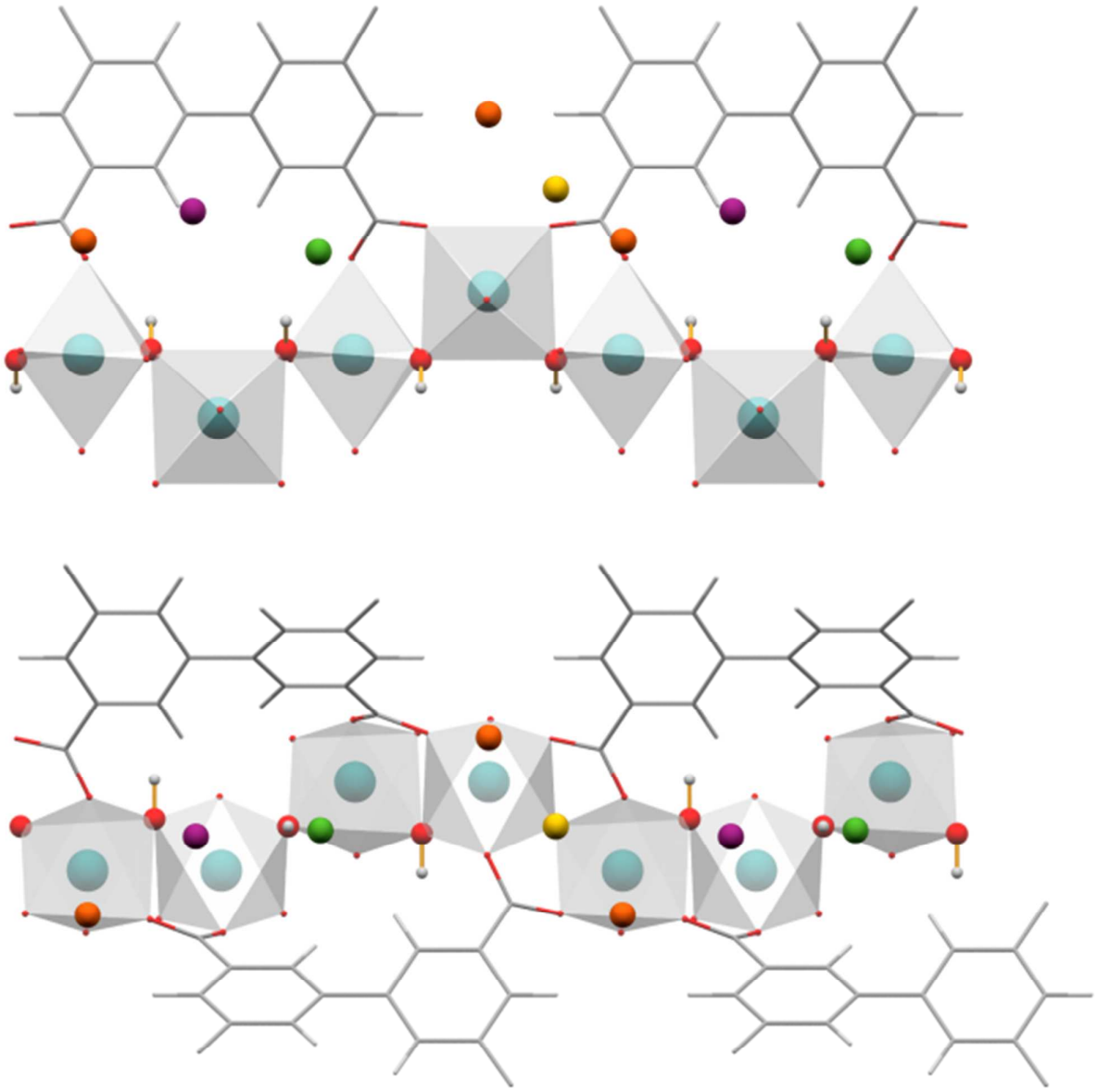

Figure S36 Two views of the *c* crystallographic axis of MFM-300(In) at a gas loading of 2.99 D_2 per In ($[In_2(OH)_2(C_{16}H_6O_8)]\cdot 5.98\ D_2$), highlighting the CD_4 binding sites (Site I, green; Site II, orange; Site III, yellow; Site IV, purple).

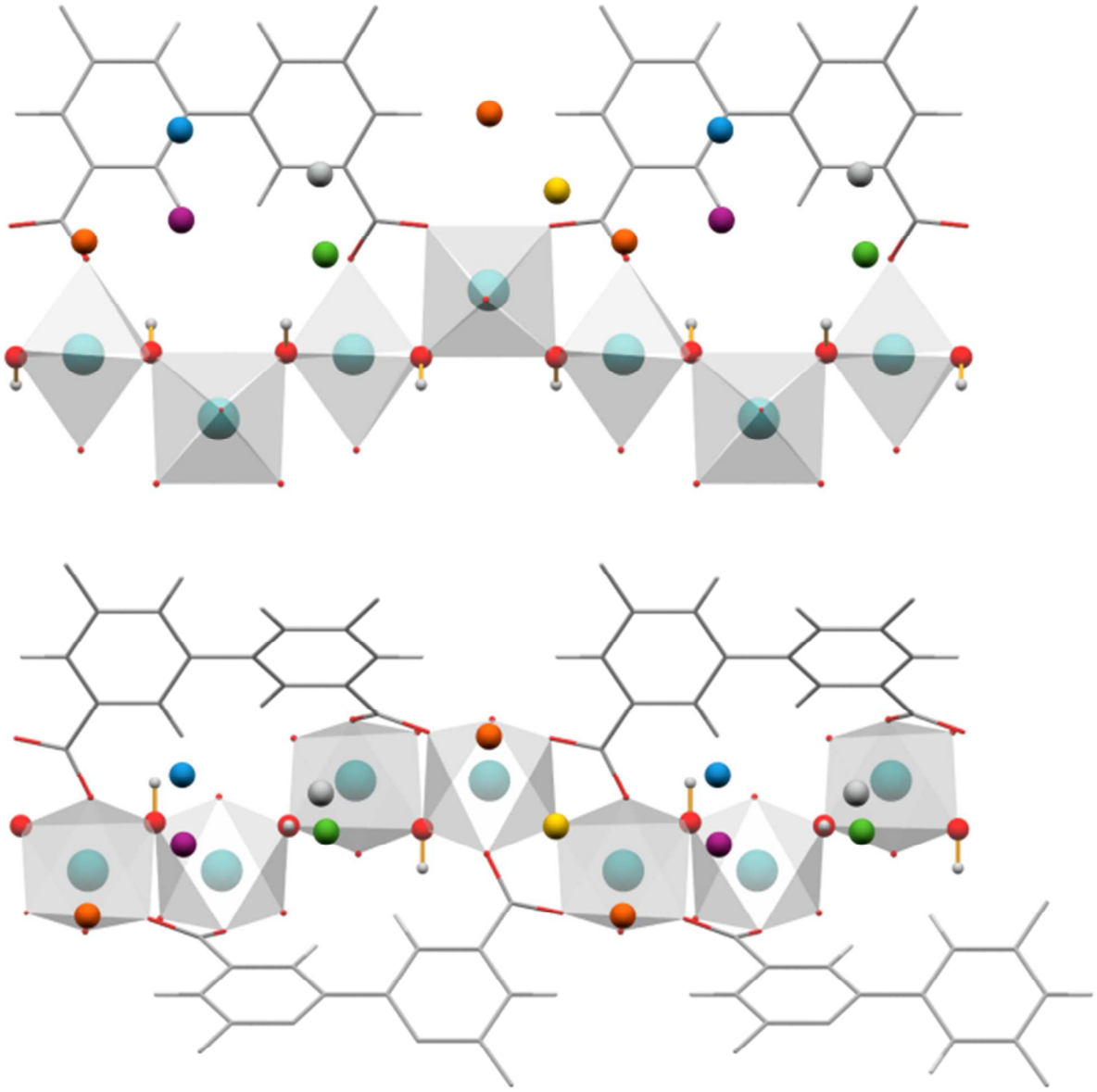

Figure S37 Two views of the *c* crystallographic axis of MFM-300(In) at a gas loading of 4.83 D_2 per In ($[In_2(OH)_2(C_{16}H_6O_8)]\cdot 9.66\ D_2$), highlighting the CD_4 binding sites (Site I, green; Site II, orange; Site III, yellow; Site IV, purple, Site V, blue, Site VI, grey).

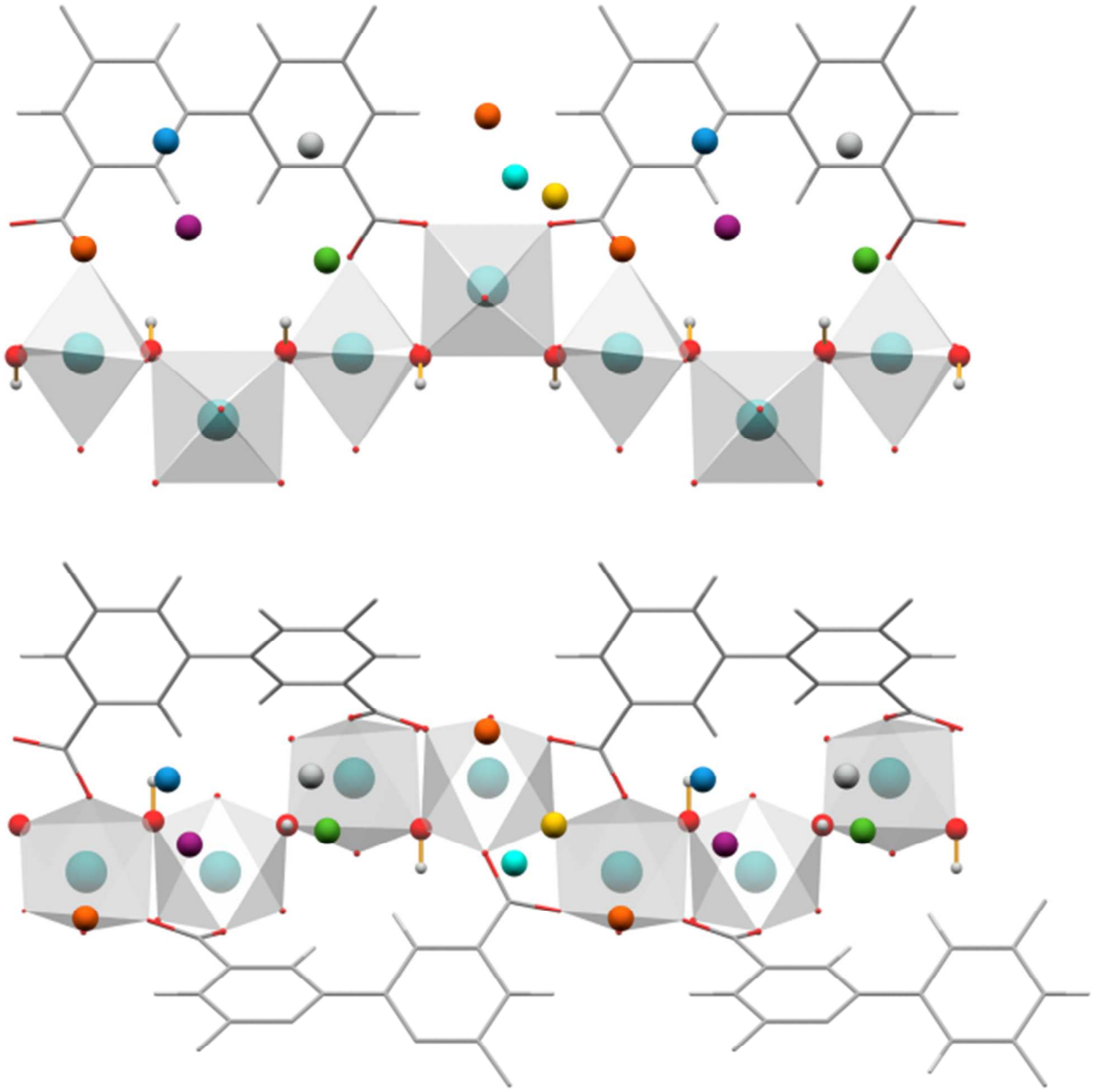

Figure S38 Two views of the *c* crystallographic axis of MFM-300(In) at a gas loading of 6.08 D_2 per In ($[In_2(OH)_2(C_{16}H_6O_8)]\cdot 12.16\ D_2$), highlighting the CD_4 binding sites (Site I, green; Site II, orange; Site III, yellow; Site IV, purple, Site V, blue, Site VI, grey, Site VII, light blue).

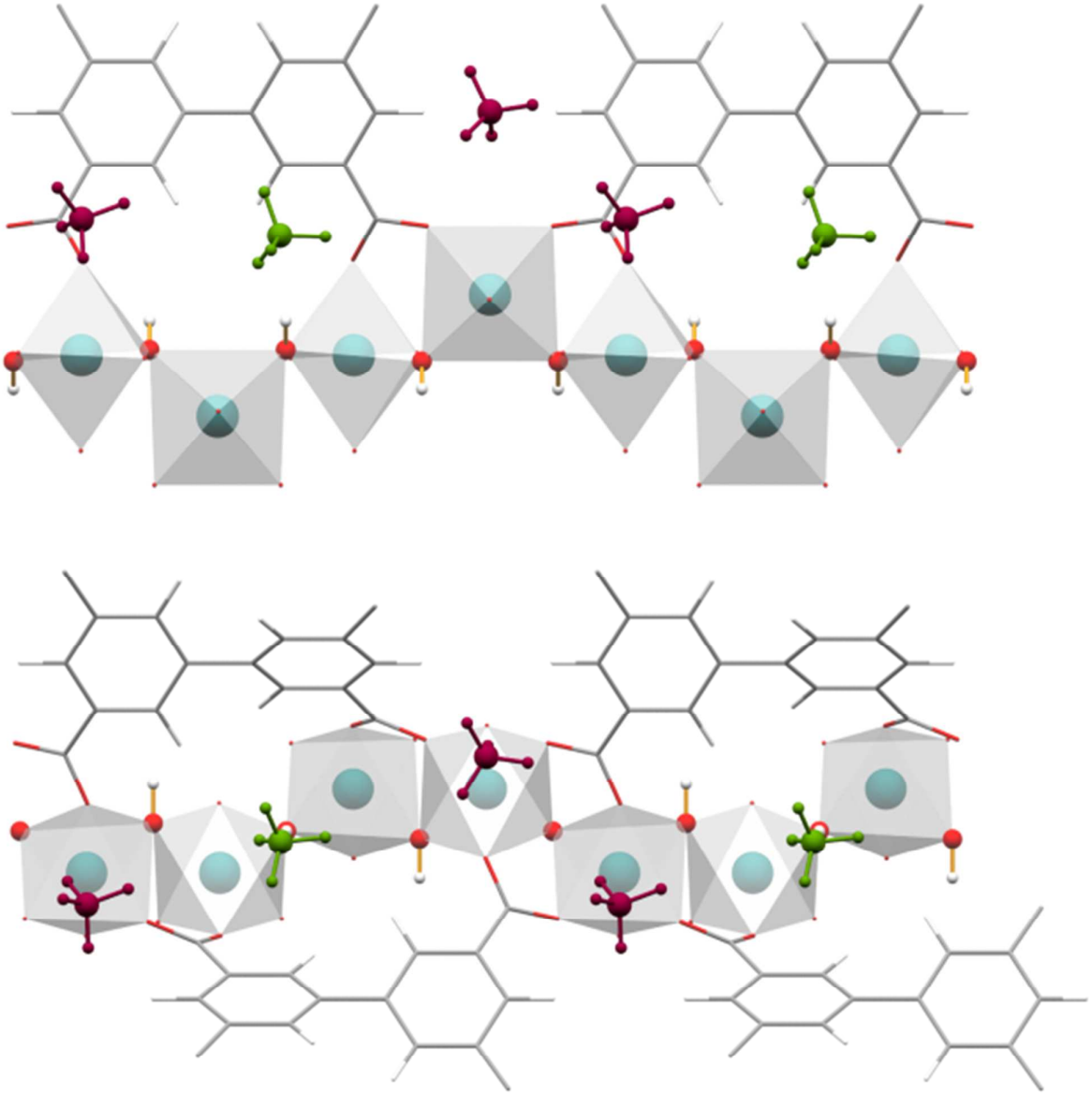

Figure S39 Two views of the *c* crystallographic axis of MFM-300(In) at a gas loading of 1.09 CD_4 per In ($[In_2(OH)_2(C_{16}H_6O_8)]\cdot 2.18CD_4$), highlighting the CD_4 binding sites (Site I, green; Site II, red).

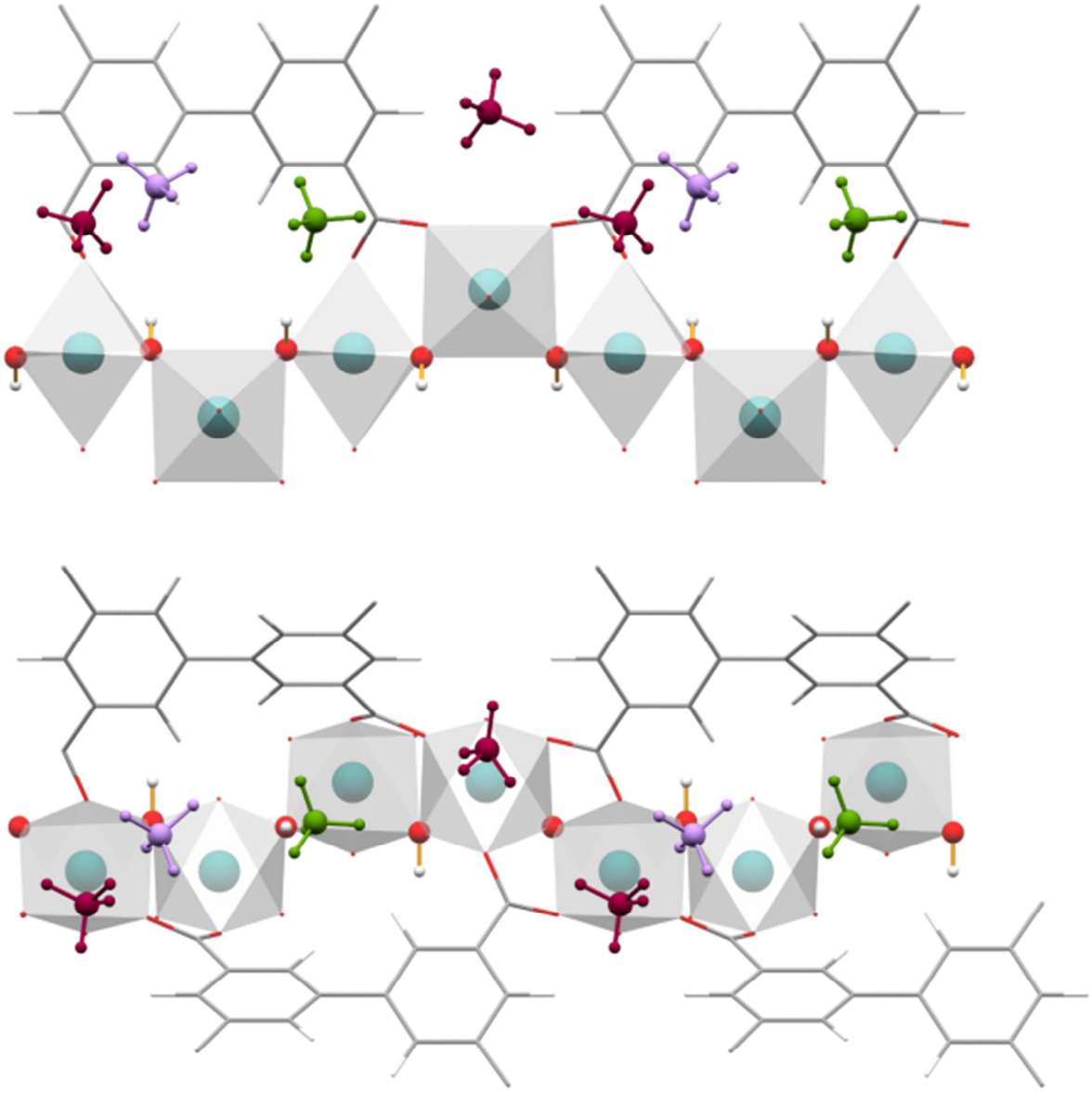

Figure S40 Two views of the *c* crystallographic axis of MFM-300(In) at a gas loading of 2.09 CD_4 per In ($[In_2(OH)_2(C_{16}H_6O_8)]\cdot 4.18CD_4$), highlighting the CD_4 binding sites (Site I, green; Site II, red; Site III, purple).

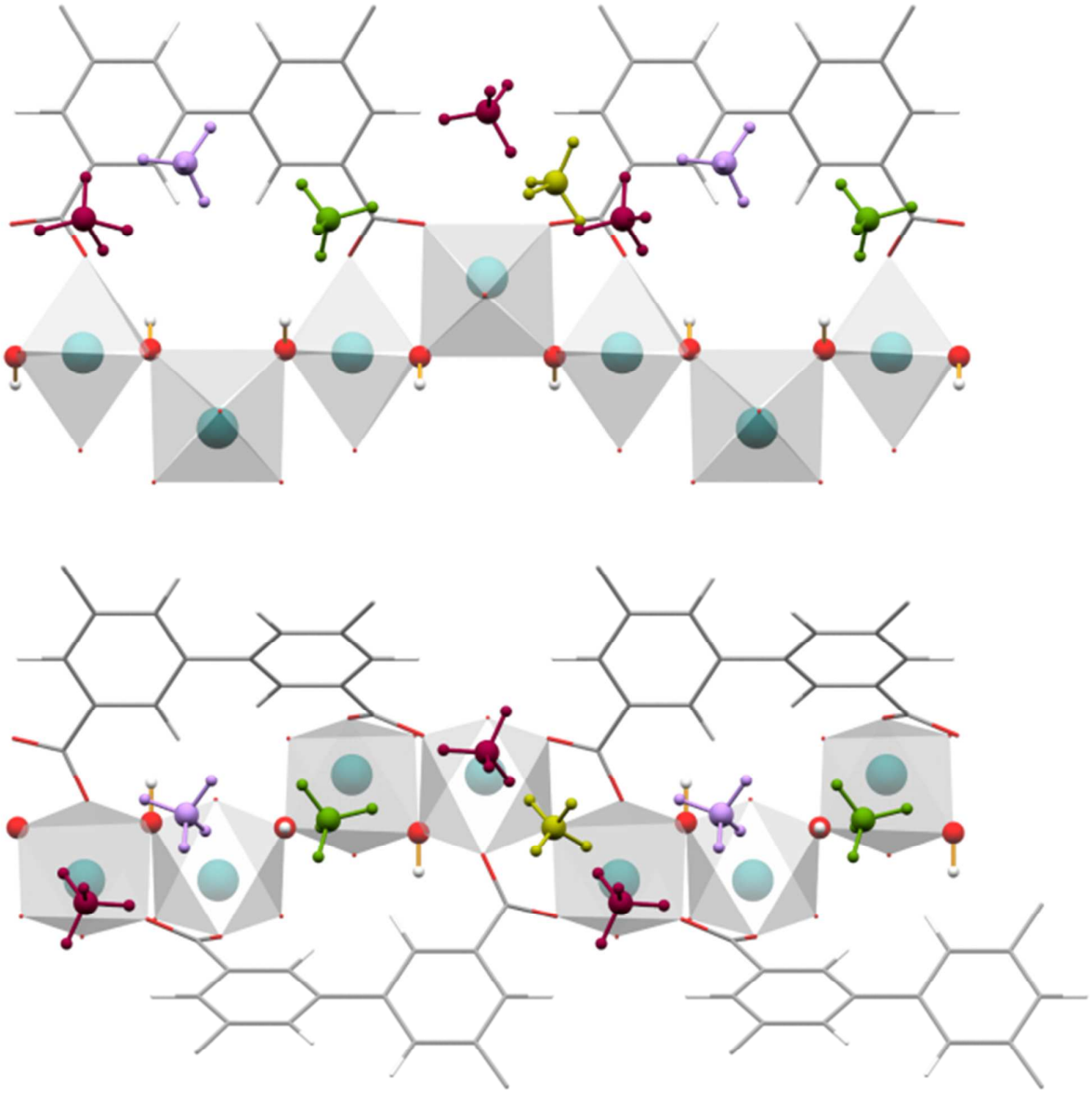

Figure S41 Two views of the *c* crystallographic axis of MFM-300(In) at a gas loading of 3.11 CD_4 per In ($[In_2(OH)_2(C_{16}H_6O_8)]\cdot 6.22CD_4$), highlighting the CD_4 binding sites ((Site I, green; Site II, orange; Site III, yellow; Site IV, purple, Site V, blue, Site VI, grey, Site VII, light blue).).

Neutron Scattering Measurements

Inelastic Neutron Scattering experiments were carried out at TOSCA,[9] a general purpose inelastic neutron spectrometer at the first target station of the ISIS Facility at the Rutherford Appleton Laboratory (UK).[6] TOSCA is an indirect geometry spectrometer situated 17 m downstream of a 300 K poisoned water moderator, comprised of 130 ^{3}He detectors in forward and backscattering geometry able to cover the whole range of molecular vibrations from 0 – 4000 cm^{-1}.

A sample of desolvated MFM-300(In) was loaded into a cylindrical vanadium sample container with an indium vacuum seal and connected to a gas handling system. The sample was degassed at 10^{-7} mbar and 100 °C for 1 day to remove and remaining trace guest water molecules. The temperature during data collection was controlled using a helium cryostat (11 ± 0.2 K). D_2 and CD_4 were dosed at 50 and 150 K respectively to ensure that the compound of interest was present in the gas phase when not adsorbed inside the crystalline structure of MFM-300(In). The sample was dosed from a calibrated volume to 1.0, 2.0, 4.0 and 6.0 H_2 per In and 0.5 and 1.0 CH_4 per In. The sample was then slowly cooled to 7 K to ensure the analysis gas was completely adsorbed with no condensation within the cell, sufficient time was then allowed to reach thermal equilibrium and data collected. The adsorbed gas was removed by heating the sample cell to 373 K, accompanied by returning the adsorbed gas to the dosing volume. When 95 % of the dosed gas had been returned, the sample was connected to a turbomolecular pump and degassed at 10^{-7} mbar and 373 K for two hours to ensure complete removal of the adsorbed gas.

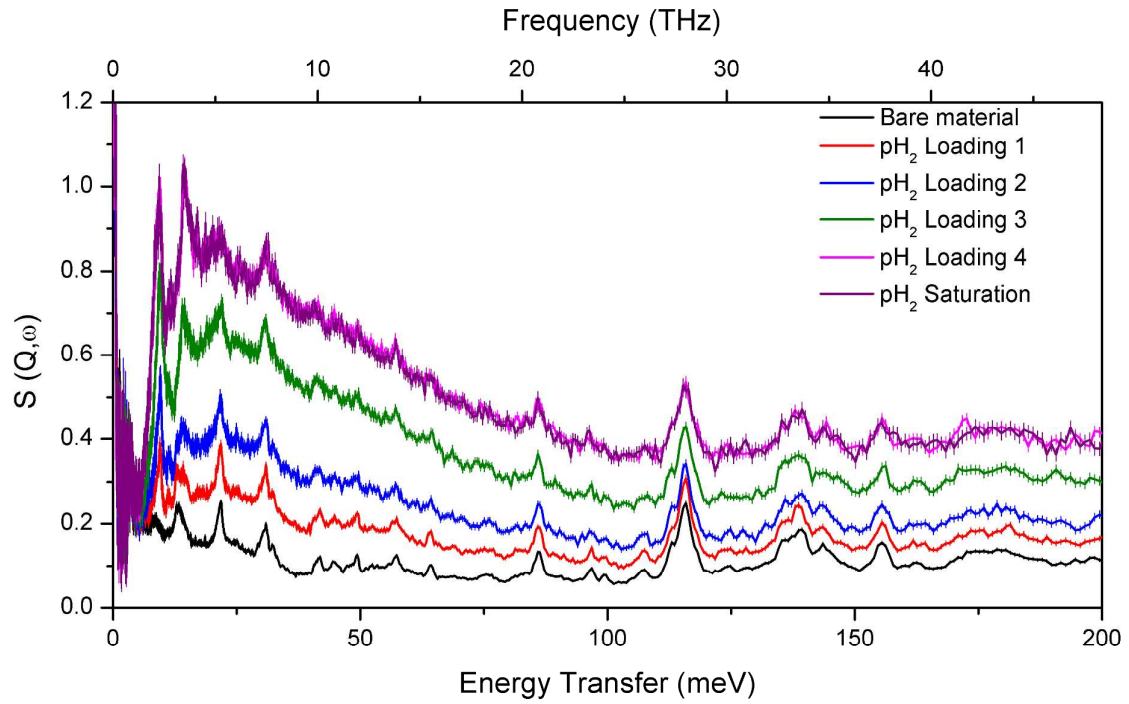

Figure S40 Comparison of the INS spectra of MFM-300(In) for the bare material and at loading of 1.0, 2,0, 4.0 and 6.0 H_2 per In.

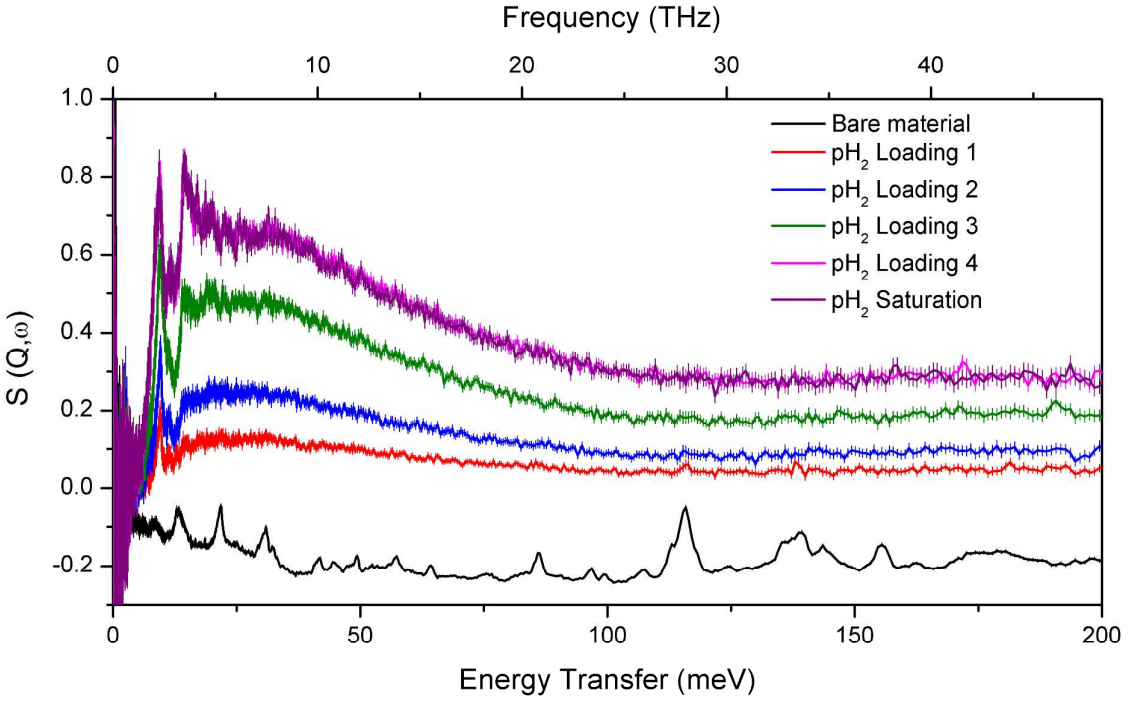

Figure S41 Comparison of the difference INS spectra for MFM-300(In) at loadings of 1.0, 2.0, 4.0 and 6.0 D_2 per In, with the bare material shown at an offset for clarity.

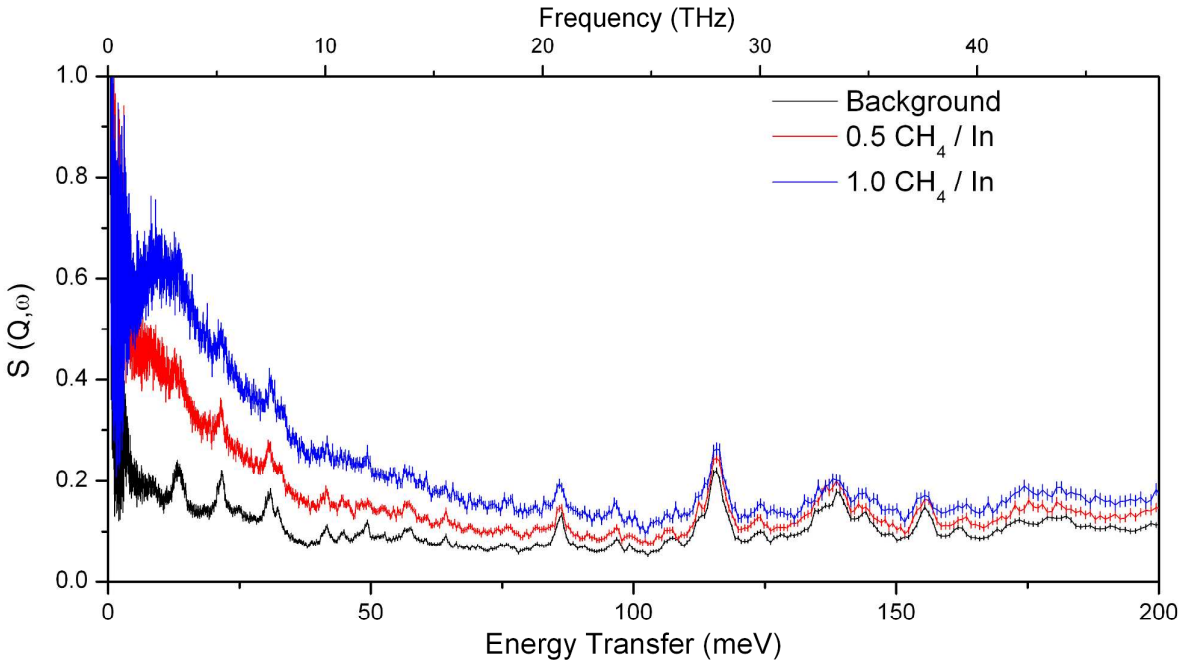

Figure S42 Comparison of the INS spectra for MFM-300(In) for the bare material, and loadings of 0.5 and 1.0 CH_4 per In.

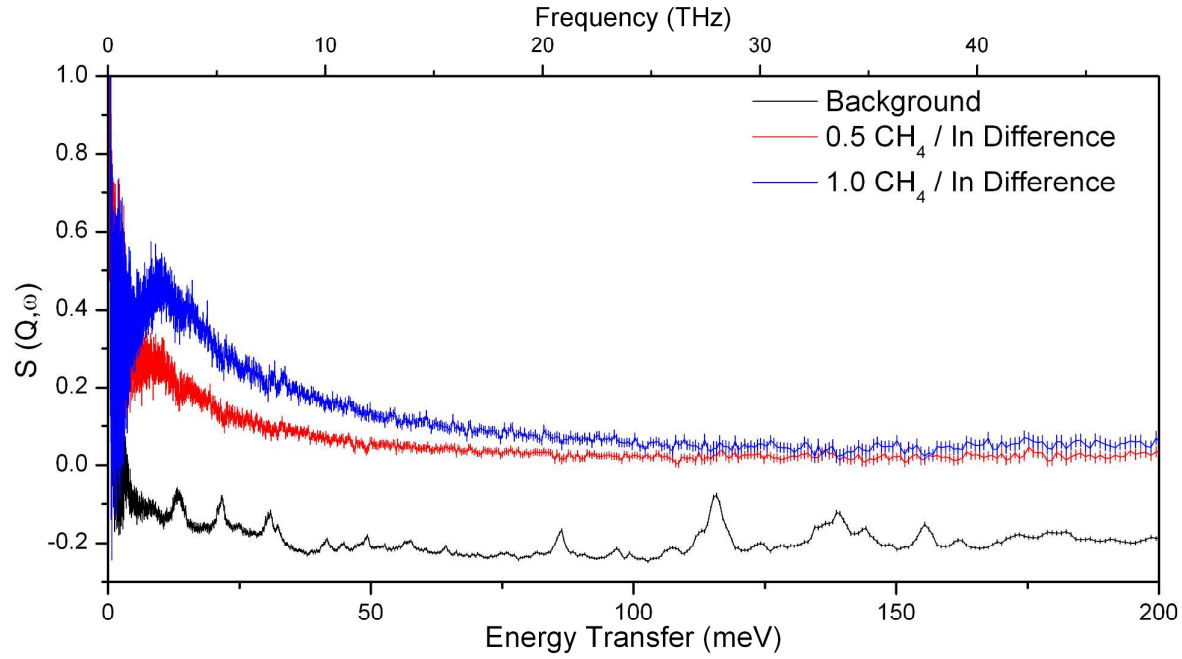

Figure S43 Comparison of the difference INS spectra for MFM-300 (In) at loadings of 0.5 and 1.0 CH_4 per In, with the bare material shown on an offset for clarity.

Molecular Dynamics Modelling of Inelastic Neutron Spectroscopy (INS)

MD simulations were performed at temperatures ranging from 50 to 250 K. The 250 K simulation was found to give the most appropriate sampling of the potential energy surface (PES) and therefore a hydrogen vibrational density of states in good agreement with the LD calculation and INS experiment was obtained (Figure 5). MD simulations of the CH_4-loaded MOF allow the vibrational density of states of the CH_4 molecules to be determined.

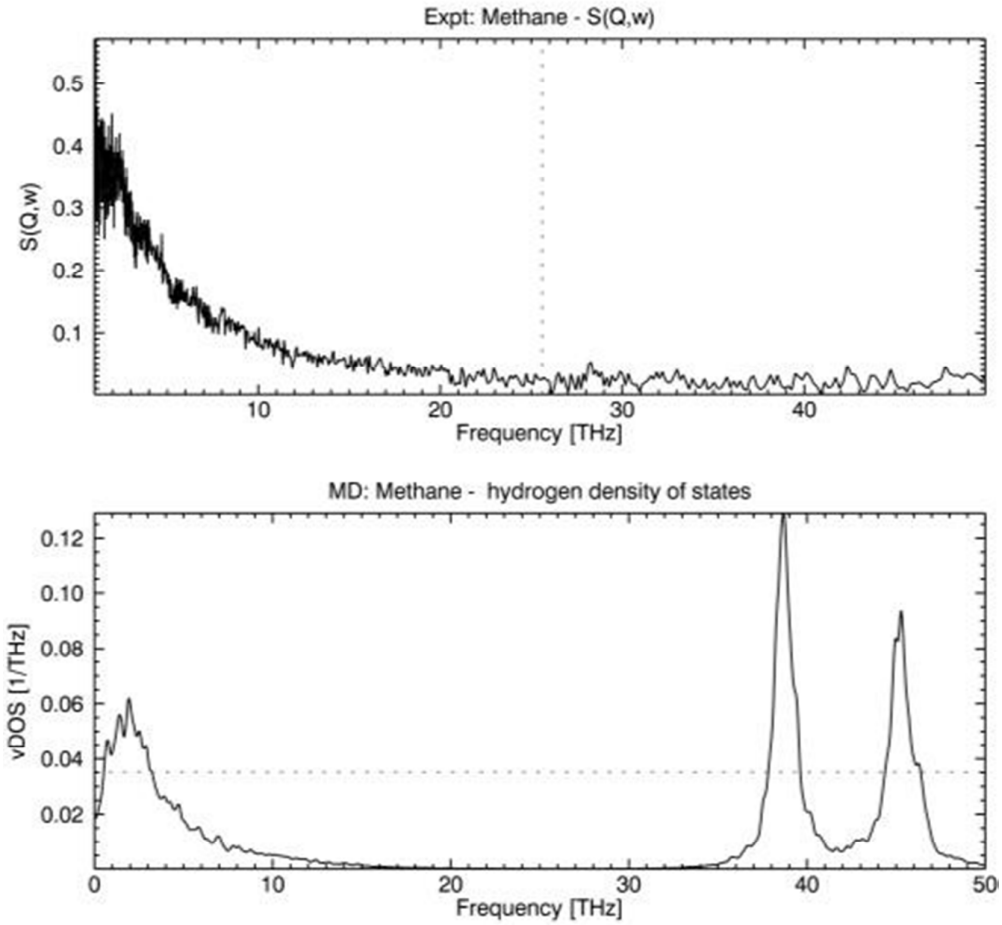

Figure S44 Comparison of the experimental difference INS spectra (top) with that of the calculated spectra (bottom).

References

1. Thompson S. P.; Parker, J. E.; Potter, J.; Hill, T. P.; Birt, A.; Cobb, T. M.; Yuan, F.; Tang, C. C. *Rev. Sci. Instrum.* **2009**, 80, 075107.
2. Rietveld, H. M. *J. Appl. Crystallogr.* **1969**, 2, 65.
3. Gupta, A.; Chempath, S.; Sanborn, M. J.; Clark, L. A.; Snurr, R. Q. *Mol. Simul.* **2003**, 29, 29.
4. Martin, M. J.; Siepmann, J. I. *J. Phys. Chem. B.* **1998**, 102**,** 2569.
5. Rappe, A. K.; Casewit, C. J.; Colwell, K.S.; Goddard III, W. A.; Skid, W.M. *J. Am. Chem. Soc.* **1992**, 114, 10024.
6. Perez-Pellitero, J.; Amrouche, H.; Siperstein, F. R.; Pirngruber, G.; Nieto-Draghi, C.; Chaplais, G.; Simon-Masseron, A.; Bazer-Bachi, D.; Peralta, D.; Bats, N. *Chem.-Eur. J.* **2010**, 16, 1560.
7. Peng, D.-Y.; Robinson, D. B. *Ind. Eng. Chem. Fundamen.* **1976**, 15, 59.
8. Chapon, L. C.; Manual, P.; Radelli, P. G.; Benson, C.; Perrott, L.; Ansell, S.; Rhodes, N. J.; Raspino, D.; Duxbury, D.; Spill, E.; Norris, J. *Neutron News* **2011**, 22**,** 22.
9. Colognesi, D.; Celli, M.; Cilloco, F.; Newport, R. J.; Parker, S. F.; Rossi-Albertini, V.; Sacchetti, F.; Tompkinson, J.; Zoppi, M. *Appl. Phys. A-Mater.* **2002***,* 74, S64.